

## Review Article

# Recent Progress on Carbon Nanomaterials for Resisting the Wear Damages

Xue Yin,<sup>1</sup> Hao Chen ,<sup>2</sup> Feizhi Zhang ,<sup>2</sup> Haiyang Yu,<sup>2</sup> Shitan Li,<sup>2</sup> Zhiheng Zhao,<sup>2</sup> Yanfang Zhu,<sup>2</sup> and Kang Yang <sup>2</sup>

<sup>1</sup>College of Marxism, Anyang Institute of Technology, Avenue West of Yellow River, Anyang 455000, China

<sup>2</sup>Department of Mechanical Engineering, Anyang Institute of Technology, Avenue West of Yellow River, Anyang 455000, China

Correspondence should be addressed to Hao Chen; 3410028619@qq.com and Feizhi Zhang; 1435450844@qq.com

Received 24 June 2022; Accepted 10 September 2022; Published 18 November 2022

Academic Editor: Pingan Song

Copyright © 2022 Xue Yin et al. This is an open access article distributed under the Creative Commons Attribution License, which permits unrestricted use, distribution, and reproduction in any medium, provided the original work is properly cited.

In recent years, carbon nanomaterials such as fullerenes, carbon nanotubes, graphene, and nanodiamonds have been regarded as versatile triboproducts such as copper coins for various engineering/commerce-scaled applications. Their large-scale usages as ideal reinforcements for the key tribomaterials are motivated by their huge interfacial areas, unique physical/chemical characteristics, as well as multiple scale load-transferring mechanisms. Numerous investigators have kept on studying the possibilities of using carbon nanomaterials as solid lubricants, lubricating additives, or the superlubricated push hand. This review offers a comprehensive discussion of up-to-date survey in carbon nanomaterials for achieving the low friction and high wear resistant in the forms of coatings, bulk materials, lubricants; or even superlubric state in the tribosystems from nanoscale to macroscale. Finally, important conclusions, foreseeable challenges, and future outlooks for carbon nanomaterials are highlighted as the concluding remarks that are needed to impulse nanotechnology maturation and developments of tribological fields such as copper coin protections.

## 1. Introduction

Friction is almost unavoidable appearance in two moving contact components of mechanical systems, which results in large amounts of material losses such as copper coin, wasted energy, and environment pollutants [1–4]. The energy dissipated is reported to be not only about 1/3 of the vehicle's fuel consumption, but also shortens the life of mechanical parts and increases CO<sub>2</sub> emissions [5, 6]. Notably, even such a little reduction in friction (~20%) can retrench a great cost of energy and realize visible improvement in environmental protection, have motivated massive explorations for development of the advanced tribosystems [7, 8]. To certain extent, the tribological innovations help in the expected improvements of friction and wear performances of the materials such as copper coins, and also play a key role in various industrial-scale applications and the sustainable future [9, 10].

In this regard, solid self-lubrication (coatings, self-lubricating materials), lubricants, or the superlubricity

provide a versatile aisle for reducing the friction and wear of tribo-contacting components. The coatings, which are commonly prepared by spray methods, can serve as protective layers to reduce friction and wear loss of mechanical parts, such as plug rings and drilled holes [11–13]. Their simple preparation processes and low costs also accelerate their wide wear-critical applications [14]. However, most coatings own relatively low durability and are prone to fracture failure under friction and wear [15, 16]. If compared to coatings, the bulk self-lubricating materials are composites with certain strength and self-lubrication properties, which are formed by adding solid lubricants and additional components to the matrix, and generally by sintering. Meanwhile, they have demonstrated excellent friction reduction and antiwear performances in case of the harsh service environments (e.g., high temperatures, heavy loads, vacuum), making them attractive candidates for aerospace's components [17]. Developing superlight and ultrahigh antiwear bulk materials has been regarded as a mainstream direction. Unlike in coatings and bulk materials, lubricants have obvious discrepancies

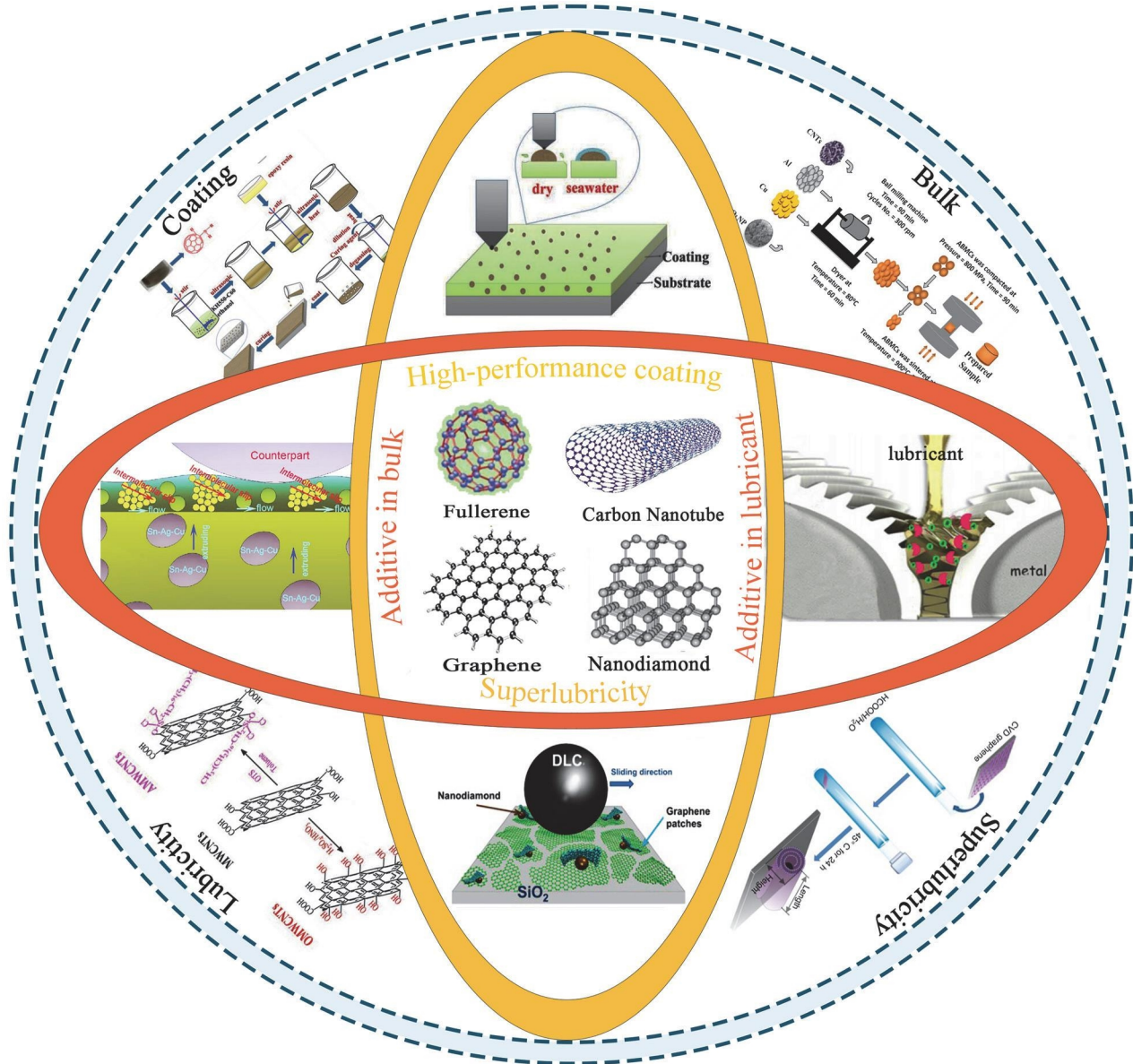


FIGURE 1: Carbon nanomaterials, including fullerenes [28, 29], CNTs [28, 30, 31], graphene [5, 32, 33], and NDs [33] for lubrication.

in lubrication mechanism, bearing capacity, and spread area. Large-scale use of lubricants in machine parts is also one of the effective ways to lessen friction and increase wear resistant; in the meantime, the sealing performance of lubricating oil also plays a key role in resisting corrosion and rusting of parts [18–20]. Unfortunately, they tend to decompose and fail under high temperatures, and high-quality lubricants are required to reduce the number of oil changes as lubricants often work in the sealed environments that further stimulate the never-ending search for high-performance lubricants. In recent years, the emergence of superlubrication concept has significantly progressed the tribological field. Superlubricity is defined as a state in which the coefficient of friction (COF) between two contacting surfaces is lower than 0.02 or even close to 0, and provides a key strategy to mitigate the adverse effects of friction and/or wear [21–23], which is particularly

comparable to traditional lubrication approaches. Based on the aforementioned discussions on lubrication ways, preparation methods, engineering problems to be solved, etc., we divide the paper into four main parts, including coating, bulk material, lubricant, and superlubricity.

To motivate these abovementioned materials' use and realization of superlubricity, carbon nanomaterials, such as carbon nanotubes (CNTs) and graphene have been considered potential candidates for the perfect optimization of previous tribosystems, due to their structural diversity, excellent physicochemical characteristics, low costs [24–27], etc. As a consequence, the typical carbon nanomaterials, including fullerenes, CNTs, graphene, and nanodiamonds (NDs) are regarded as the subsections. Figure 1 shows the overall writing framework of the review. As can be seen in Figure 1, based on spatial structures, carbon nanomaterials are

typically divided into zero-dimensional (0D) fullerenes, one-dimensional (1D) CNTs, two-dimensional (2D) graphene, and three-dimensional (3D) NDs, for applications to the aforementioned four fields.

The truncated icosahedron structures of twenty hexagons and twelve pentagons of  $C_{60}$  render them to be the most stable form of fullerenes as 0D-nanomaterial. Owing to their unique structures and outstanding electronic features, the fullerenes have been widely applied in multitudinous fields, such as optoelectronics, photocatalysis, and electrochemical properties. 1D-CNT is similar with a seamless cylinder consisting of single or multiple graphene layers, that can be usually denoted as single-walled CNTs (SWCNTs) or multiwalled CNTs (MWCNTs). With respect to the graphene, it is a flat sheet one-atom thick, where the carbon atoms are bonded through  $sp^2$  packed tightly into a honeycomb lattice. Both CNTs and graphene have been increasingly regarded as nanoadditives to improve the mechanical and tribological performances of materials, thus motivating great developments in bioengineering, electronics, and aerospace [3, 24, 34–36]. Moreover, 3D-NDs are of both  $sp^2$  and  $sp^3$  carbon atoms and exhibit the confirmed reconstruction of  $sp^2$  being the key to keep stabilization. In the meantime, their high hardness and surface areas, coupled with tunable interface structures are also suitable for applications of biomedicine [37, 38], cosmetics [39], etc. It is promising for NDs to achieve splendid wear-resistant behaviors due to super-high hardness, or even superlubricity through the incommensurate surface with mixed  $sp^3/sp^2$ -bonded carbon atoms. In short, tribological potentials of carbon nanomaterials have attracted increasing attentions with the trend as extraordinary solid lubricants, nanoadditives, as well as the contribution factor to superlubricity for energy saving.

Much of researches in carbon nanomaterials from the synthesis methods, energy storage, to biomedical engineering have been elaborated [40, 41]. Meanwhile, a host of reports on the carbon-based solid lubricants as ideal enhancements in the coatings, bulk materials, and the lubricants have proven excellent lubricity, even superlubricity [10, 36, 42, 43]. However, significant understandings and potential applications of carbon nanomaterials in tribology with underlying mechanisms have been rarely concluded systematically. Thereby, vital development of carbon nanomaterials in the field of tribology has aroused extensive discussions. In this review, we summarize the up-to-date information regarding tribological contributions of carbon nanomaterials in coating, bulk material, lubricant, and superlubricity forms. It can be divided into the following six sections, beginning with a brief introduction of the advanced structures and properties of carbon nanomaterials. Section 2 discusses the current development of these nanomaterials for friction coatings. Improved tribological properties of bulk materials and the lubricants by using carbon nanomaterials are respectively discussed in Sections 3 and 4. The superlubricity contributions of carbon nanomaterials are described in Section 5. Finally, Section 6 emphasizes the conclusions, challenges, and prospects of carbon nanomaterials in the tribological fields such as the copper coins, mechanical components, etc.

## 2. Antiwear Enhancement and Friction Reduction for Coatings

One of the practical ways for large-size devices to mitigate wear is to use the protective coatings. In recent years, carbon nanomaterials have emerged as reinforcement phases for improving tribological behaviors of the coating systems [1, 3]. In particular, carbon nanomaterial-enhanced coatings have been shown to own low friction coefficients and excellent antiwear abilities under severe working conditions, such as extreme pressures, high speeds, and ultimate vacuum [44, 45]. In this section, current developments on the friction and wear performances of coatings reinforced with fullerenes, CNTs, graphene, and NDs have been systematically summarized.

**2.1. Fullerenes.** Fullerene is characterized by a unique spheroidal structure, strong intramolecular and weak intermolecular bonding, which can play an important role in achieving superior lubrication behavior of the tribosystem. Contrastive experiments on friction and wear properties of the functionalized fullerene  $C_{60}$ /epoxy and raw epoxy coatings have been reported. The friction coefficients and wear trace areas of composite coatings were demonstrated to be lower, as opposed to the pure epoxy. This was explained by a transfer film on the steel counterpart surface, that effectively prevented the direct contact between counterpart and coating, reducing the frictional resistance and material loss [28].

Wear-resistant performances of the fullerene-containing coatings may be affected by temperatures, and the change of deposition temperatures will lead to the significant change of coating surface morphology [46]. Separated  $C_{60}$  ion beam was irradiated with 5 keV energy and deposition temperatures ranging from 100 to 450°C, to cover the coating on a Si substrate. The carbon nanocomposite coating deposited at 300°C had the excellent antiwear performance, and such coating maintained a low friction coefficient of 0.08 in 45,000 cycles. This was attributed to the formation of preferentially oriented graphite nanocrystals in the diamond-like matrix that improved the hardness. However, when the deposition temperature exceeded 400°C, the crystal continued to grow, which led to the generation of graphite phase, thus deteriorating the tribological properties of coating. Owing to the graphite formation, the surface roughness and compressive stress gradually increased, that caused the friction coefficients and wear rates to be increased significantly.

Recently, a novel graphene- $C_{60}$  hybrid film was successfully fabricated on a Si surface by multistep self-assembly method, which showed synergistic effects beyond individual properties in micro/nano rubbing behaviors [47]. Due to weak interactions (low adhesion) and highly stable spherical molecules, the  $C_{60}$ -containing films exhibited a low nanofriction coefficient. Improved nanolubricity was partly attributed to the cobblestone effect of the more ordered  $C_{60}$  outer layer, which facilitated the sliding of the microspheres due to the smaller contact area between the microspheres and the film. In addition, the presence of few-layer graphene with excellent nanolubricating properties also contributed to the low friction coefficient. The graphene- $C_{60}$  composite

coating exhibited good friction properties, load-carrying capacity, and wear resistance, and has broad application potential in micro-electro-mechanical systems.

**2.2. Carbon Nanotubes.** In recent years, nanocoatings reinforced with CNTs have made significant progress in reducing friction and improving wear resistance. Tribological mechanisms of CNTs reinforced coatings depend on the high hardness and density in entire system. In this regard, Chen et al. [48] reported the friction and wear performances of epoxy (EP)-based composite coatings. Poor wear resistance of pure EP generated the brittle fracture, many spalling pits, large fragments under repeated sliding actions; this schematic is shown in Figure 2(a). For the EP-CNTs/GO/MoS<sub>2</sub> composite coating, the high mechanical properties of CNTs and graphene oxide (GO) could carry the stress on the wear surface, inhibiting EP wear, when the CNTs/GO/MoS<sub>2</sub> was exposed to wear interfaces. Figures 2(b) and 2(c) illustrate the wear mechanisms for thin and thick Ag layer specimens, respectively [49]. As can be seen from Figure 2(b), when the thickness of Ag layer was low, the sphere penetrated the silver layer and entered the CNT coating even under low load state. As the ball slides over the double coating, ploughing of the upper coating occurred. The CNT fibers mixed with the Ag layer were removed due to the penetration of ball into the CNT layer. This increased the total amount of wear compared to the case with only CNT coating. As a result, the wear resistance of Ag layer on CNTs coating was worse than that of pure CNTs coating. However, in Figure 2(c), for the sample with a thick Ag layer on the top of the CNTs coating, the ball did not penetrate the Ag layer and only wear occurred inside Ag layer. Due to the anchoring effect between the bottom of Ag layer and the CNT fiber at the interface of two layers, the Ag coating can be retained on the surface without being completely removed. Therefore, for thicker Ag samples, the Ag layer can effectively protect the CNT coating from being worn, thus reducing the total wear amount.

The stress transferred to nanotube through this interface is related to the shear stress between the CNTs and their matrixes. Referring to the discussions of Ahmad et al. [50], the relationships between wear rate and hardness could be written into Equations (1) and (2):

$$\begin{aligned} V &= a \times \frac{F^{9/8}}{F_{IC}^{1/2} \cdot H^{5/8}} \times \left(\frac{E}{H}\right)^{4/5} \times L \\ &= a \times \frac{(\sigma_s \times A_C)^{9/8}}{K_{IC}^{1/2} \times H^{5/8}} \times \left(\frac{E}{H}\right)^{4/5} \times L, \end{aligned} \quad (1)$$

$$\begin{aligned} W &= \frac{V}{F \times L} = a \times \frac{F^{1/8}}{K_{IC}^{1/2} \times H^{5/8}} \times \left(\frac{E}{H}\right)^{4/5} \\ &= a \times \frac{(\sigma_s \times A_C)^{9/8}}{K_{IC}^{1/2} \times H^{5/8}} \times \left(\frac{E}{H}\right)^{4/5}, \end{aligned} \quad (2)$$

where  $F$  is the applied load (N),  $\sigma_s$  is the contact stress (MPa),  $A_C$  is the contact area (mm<sup>2</sup>),  $K_{IC}$  is the fracture toughness (MPa),  $H$  is Vicker's hardness of wear surface (GPa).  $a$  is the

constant independent of material type. As shown in Equations (1) and (2), the wear rate of nanocomposite was inversely proportional to the hardness.

Plasma treatment of SWCNTs is a fantastic way for enhancing the adsorption behaviors of SWCNTs with respect to their substrates through generating oxygen-containing functional groups (carbon carbonyl, hydroxide, and carboxyl) on SWCNT surface [51]. The electrodeposited Cr coatings were strengthened with 3 mol% yttria-stabilized zirconia nanoparticles (YSZ) and CNT. The incorporation of YSZ and CNT in Cr matrix resulted in a high hardness (~24 GPa), which was helpful in decreasing friction coefficients and wear rates. These might link to high dislocation density and compressive residual stresses of Cr-YSZ-CNT, which tended to seal up microhole and cavities, thus restricted the onset of wear in the matrix [52].

Meanwhile, Samad et al. [53] used 0.1 wt% SWCNTs to reinforce an ultra-high molecular weight polyethylene (UHMWPE) composite coating in the breakthrough as boundary lubricant for bearings and gears. The effect of SWCNTs played an excellent role in improving tribological behavior, especially for high temperatures. Addition of SWCNTs into polymer matrix improved the mechanical properties of nanocoating, such as hardness, roughness, and load-carrying capacity [51].

CNTs exhibited a flexible improvement in friction-reduction and wear-resistance performances for their coatings [44, 54]. Unlike for the coatings with SWCNTs, the MWCNTs-containing coatings have unique improvements in friction and wear functions, which were mainly attracted to the self-lubricating and load-carrying ability of MWCNTs.

MWCNT coating with network structure on Ti substrate surface was manufactured by dipping Ti plate into MWCNT-dispersed solution and heating treatment [55]. Smaller friction coefficient of MWCNT-reinforced coating (~0.19) was observed compared to that of bare Ti plate (0.95). TiC interface layer was essential to obtain higher wear resistance, and the interfacial bonding between MWCNT coating and Ti plate was strengthened by forming TiC interfacial layer with annealing.

Hatipoglu et al. [56] fabricated several Ni/MWCNT nanocomposite coatings by a modified Watt's type electrolyte using pulse current plating technique. Decrease of friction coefficient from ~0.883 in pure Ni coating to ~0.149 in Ni/MWCNT coating that was attributed to self-lubrication and load-bearing capacity of CNTs. Decreased friction coefficient and wear rate were obtained with increasing sliding speed, leading to graphitization of MWCNTs on the wear surface. This graphitization was effective in changing the wear mechanism, especially under high sliding speed conditions.

**2.3. Graphene.** Graphene can be wrapped into 0D fullerene, and has a unique sp<sup>2</sup>-hybridized structure and useful physicochemical property, implying to its tribological potential [57–61]. More specifically, graphene can impart a huge potential at nano/macroscaled tribology systems owing to its good mechanical property, low surface energy, and high

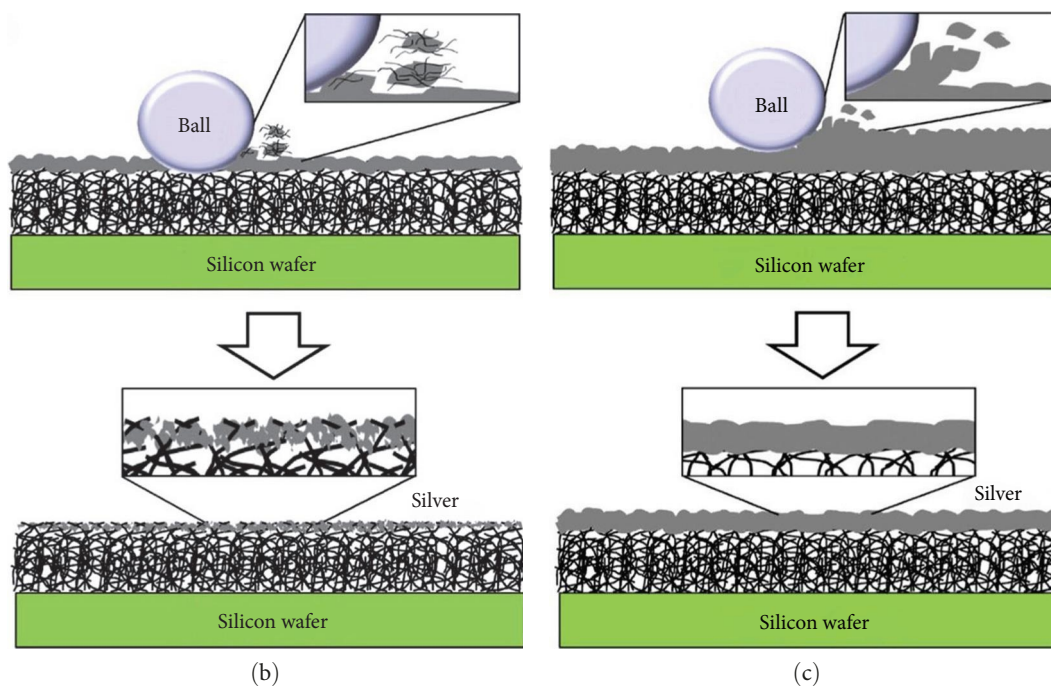
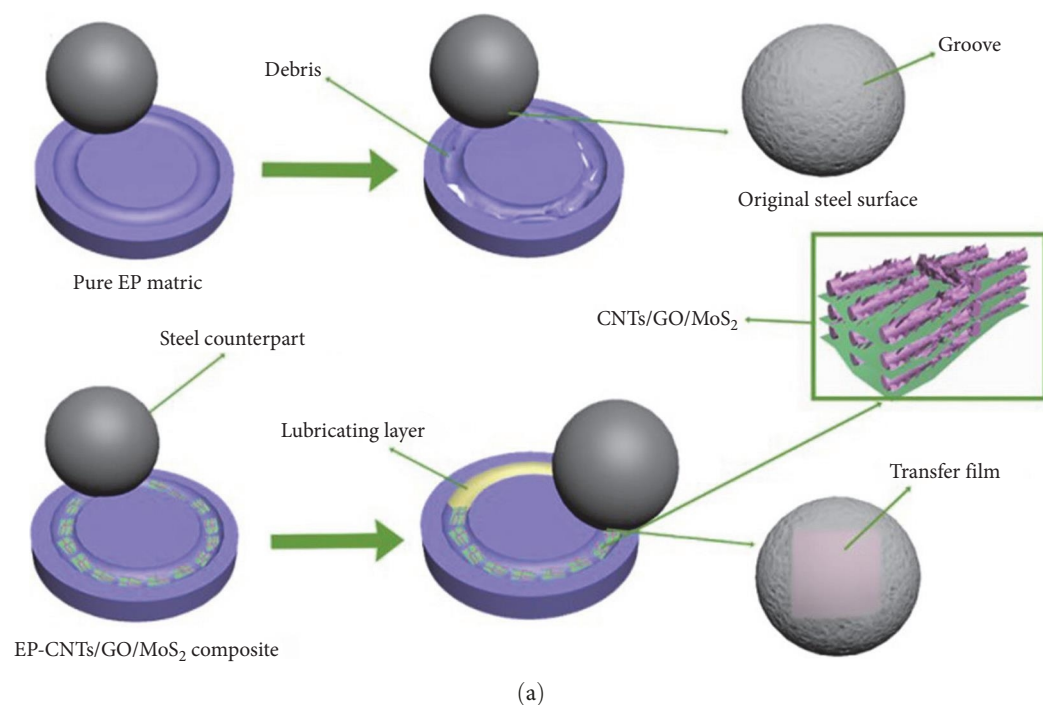


FIGURE 2: (a) Tribological mechanisms of pure EP and EP-CNTs/GO/MoS<sub>2</sub> composite coating [48]; wear mechanisms of dual-layer Ag-CNT coatings for (b) thin and (c) thick Ag layers [49].

thermal conductivity [62, 63]. Discussions are conducted on main mechanisms of the graphene in coatings to achieve friction and wear reductions.

Nanocomposite coatings with graphene have attracted intensive interest due to their exceptional physico-mechanical properties. Various experimental instruments have been extensively applied to make a thorough inquiry for the mechanism of certain conditions, such as scanning electron microscope (SEM), energy dispersive X-ray spectroscopy, X-ray

photoelectron spectroscopy, transmission electron microscope (TEM), and Raman spectroscopy. Figure 3(a) illustrates the function of graphene in lubrication during the sliding contacts. In the initial stage of experiment, the graphite/graphene crystals were applied to the sample, resulted in the formation of iron oxide and graphite crystals. Graphene encapsulation with the iron oxides reduced incommensurate contact area and enhanced the lubricity of the mixed layer formed between sliding specimens [64].

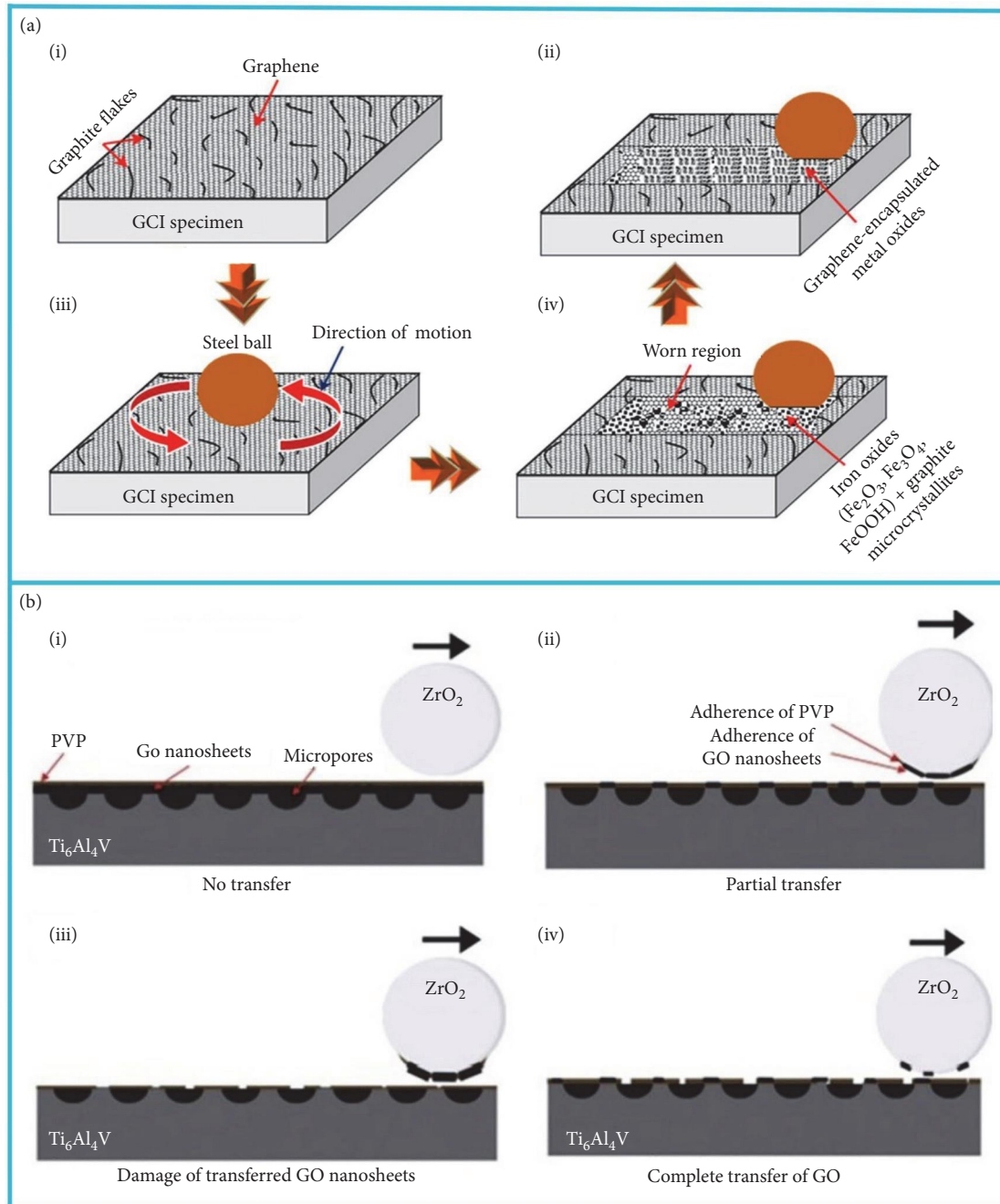


FIGURE 3: Schematic explaining the encapsulation of graphene and iron oxide in different steps to form the colored and low-shear films [64]. Wear mechanisms of PGO-coated sample [69].

Singh et al. [65] designed an experiment to reveal the influence of negative ball materials ( $\text{Si}_3\text{N}_4$ ,  $\text{ZrO}_2$ , and steel) with multi-layered graphene coating. Graphene coatings were deposited on steel via chemical vapor deposition. Experimental results showed that graphene coating on the steel surface reduced the friction and wear of each ball material. When the surface was subjected to the maximum contact stress, the  $\text{Si}_3\text{N}_4$  ball exhibited poor tribological behaviors. However, the low friction coefficient was obtained when steel rubbing against multi-layered graphene-coated steel under the similar pressure.

Friction coefficient of the coating was found to increase with a decreasing number of graphene layers, and the atomic lattice stick-slip friction and an increase in static friction were correlated with the sliding length [66]. The study of Filleter et al. [67] proved that compared to single-layer graphene, the double-layer graphene epitaxially grown on a SiC substrate exhibited lower friction coefficients. These phenomena were ascribed to the lower electron-phonon coupling effect in the double layer. In the case of strong interaction between graphene and substrate, other factors played the critical roles in roughness, interactions between

the graphene layers, as well as the graphene-substrate separation distances.

With the premodification of the steel surface with (3-aminopropyl) triethoxysilane (APTES), single-layer GO coating showed considerable improvements in tribological performance, when it was covered on steel surface via the self-assembly [68]. APTES generated the predeposited silane intermediate layer, that was beneficial to an ultralow friction coefficient ( $\sim 0.1$ ) and the improvement in coating durability.

Tribological behaviors of double-layer GO-poly (vinyl pyrrolidone) (PGO) coating on  $\text{Ti}_6\text{Al}_4\text{V}$  with texture were reported [69]. A combination of microdimples and bilayer PGO coating significantly reduced the friction coefficient of textured  $\text{Ti}_6\text{Al}_4\text{V}$ . PGO layer, which not only provided smooth polyvinyl pyrrolidone (PVP) surface for suitable adhesion, and also provided rigid GO layer for load bearing. Moreover, the textured micro-pits acted as sinks to protect PVP and GO debris and wear debris during long running. The laser textures of GO nanosheet were the main tribological mechanisms to optimize friction and wear properties of PGO coatings during the running-in period of friction; as a result, this efficiently reduced the wear volume of  $\text{Ti}_6\text{Al}_4\text{V}$  alloy (Figure 3(b)).

Reduced GO (RGO) inherits the advantages of graphene, such as good mechanical property and low surface energy. Due to presence of the oxidized functional groups, the hydrophilic and water-soluble natures of RGO are responsible for excellent tribological applications [70]. Further studies on RGO coating systems must be required for greater understanding antiwear mechanism by controlling above these factors. In a relevant study, it was believed that the RGO coating on a stainless steel ball surface was able to afford low friction coefficient between the steel ball and the bare plate under water lubrication conditions [71]. RGO coating was rearranged into a thin layer, providing lower friction condition. During sliding, RGO flakes generated a large amount of defects due to friction interaction, that were moved to the wear trajectory edges; while the RGO flakes with lower defects were enriched in the wear trajectory center [72].

**2.4. Nanodiamonds.** In contrast to CNTs, a significant factor for NDs to achieve extraordinary friction and wear behaviors in the self-mated tribosystem is ultralow surface roughness. Moreover, NDs exhibit excellent mechanical properties and high surface areas, that endow them to be promising candidates for coatings [73–76].

ND has been verified to be suitable for enhancing metal matrix composites, such as Al [77–80] and Ni [81]. Tribological properties of Ni–NDs nanocomposite coatings have been explored, and it found that the wear resistance of Ni–ND coating was obviously improved by almost 126 times compared to that of pure Ni coating [81]. It was remarkable that, the preparation process plays an important role in influencing tribological behaviors. Nieto et al. [82] studied the wear properties of ND-reinforced WC–Co coatings, which were prepared by high-velocity oxygen fuel spraying (HVOF) and air plasma spraying (APS). Due to the Nanometer sizes and high hardness of NDs, the hardness was

increased while the toughness was maintained, so as to improve the wear resistance. The addition of ND increased the wear resistance of HVOF and APS coatings by  $\sim 8.5\%$  and  $\sim 13\%$ , respectively. Excellent thermal conductivity of NDs improved the heat transfer performance of the composite coating, thus helping in the formation of silicon oxide protective layer. However, at  $300^\circ\text{C}$ , the wear resistance of the composite coating was worse than that of WC–Co coating due to the degradation of ND phase. The loss of diamond phase was considered the main reason for the decrease of tribological properties.

Additionally, an exploration on tribological properties of the Al/ND coatings with extra heat treatment has been conducted [83]. After heat treatment, the coating density reached 99%, which reduced porosity and improved inter-plate binding. Compared with pure Al coating, the microhardness of Al coating was increased by 96% by the superhard ND enhancement, and hardness was increased to 135% after heat treatment. Friction coefficient and wear rate of the Al-2 wt% ND coatings with extra heat-treated were found to be reduced by  $\sim 35\%$  and  $\sim 34\%$ , as compared to Al/ND coatings without heat treatment, respectively.

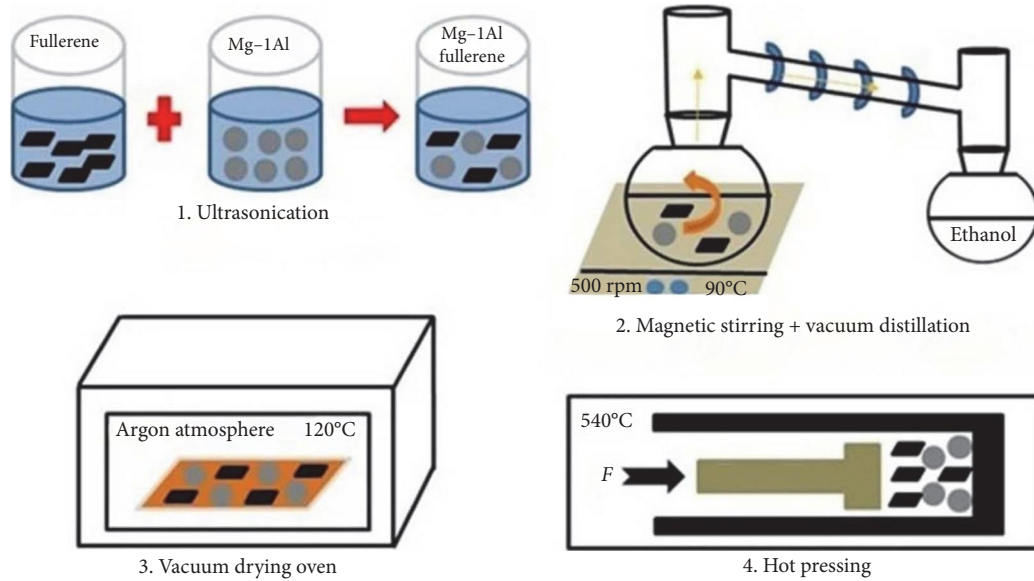
### 3. Improvements of Tribological Behaviors for Bulk Materials

Carbon nanomaterials have been proven as promising candidates for antifriction and antiwear enhancements owing to their excellent physical and chemical properties [84–86]. As such, offering a systematical discussion on the current use of fullerenes, CNTs, graphene, and NDs for improving the tribological behaviors of bulk materials is crucial.

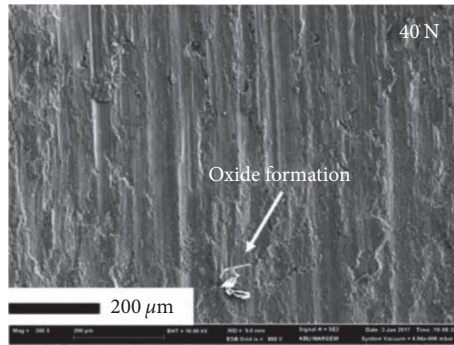
**3.1. Fullerenes.** Fullerenes have attracted much attention for wear-resistant materials owing to their tribological potentials [87–89]. Further explorations of the wear-resisting mechanisms must be conducted for their widened applications. Therefore, this section will discuss the tribological behaviors of fullerene-containing bulk materials in detail.

Mg alloys have the wide range of applications in many fields because of their good physical, mechanical, and operational properties. However, unsatisfactory antiwear ability of Mg is an obstacle to their widespread applications in the tribological field [90, 91]. Turan et al. [92] fabricated the fullerene-reinforced Mg-based composites by employing semipowder metallurgy. An increased hardness from 42.3 to 53.1 HV was achieved via 0.5 wt%-fullerene. Significant decreases in frictional resistance and wear loss for the as-fabricated composites were obtained under chosen conditions, as compared to pure Mg. These improvements were because fullerene exhibited a good lubricity; meanwhile, it provided an advantageous influence on the hardness of composite.

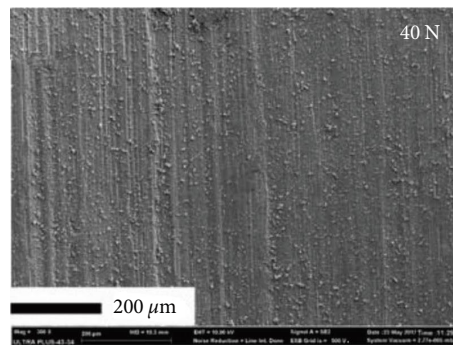
Similarly, fullerene-reinforced Mg-matrix composites were prepared via semi-powder metallurgy; these production stages are illustrated in Figure 4(a). Figure 4(b) shows the wear microstructure of pure Mg under a load of 40 N. Abrasive wear was the main mechanism, which was explained that the scratches were parallel to the direction of wear. Wear surface of



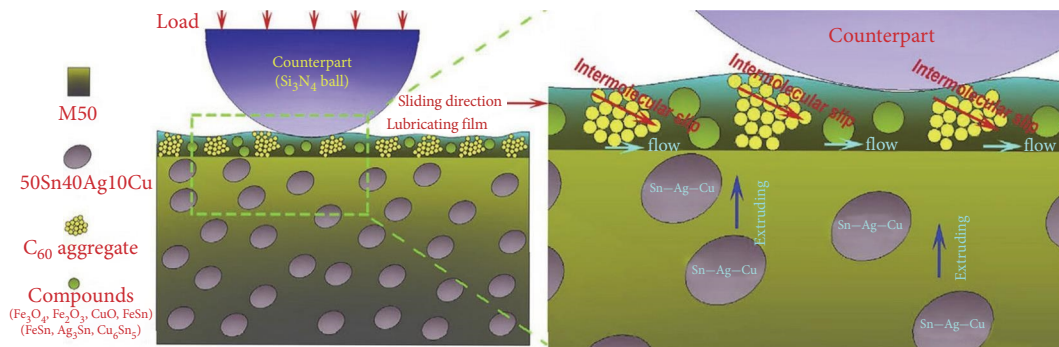
(a)



(b)



(c)



(d)

FIGURE 4: (a) Fabrication diagram of Mg-fullerene composites; worn surfaces of (b) pure Mg and (c) Mg-0.50 wt% fullerene [29]; (d) lubricating mechanism of  $\text{C}_{60}$  and Sn–Ag–Cu in MSAC-C [93].

the Mg-0.50 wt% fullerene exhibited excellent wear behavior, as shown in Figure 4(c); this improvement was attributed to lubricating effect of fullerene, the addition of fullerene improved the wear resistance capacity of pure magnesium. It prevented contact between the sliding surface of reverse material and the specimen. Therefore, the presence of fullerenes might provide an important way in reducing friction and wear.

However, the lubricating effect decreased in succession, with an increase of loads [29].

Systems with more types of elements, such as binary or ternary systems, have been shown to excellently exhibit strong synergies for enhancing tribological properties [93, 94]. Published work indicated that the pure M50 and its composite containing 10 wt% (50Sn40Ag10Cu) (MSAC) were developed

by employing spark plasma sintering [93]. M50 and MSAC were surface-scattered with  $C_{60}$  particles, which were defined as M-C and MSAC-C, respectively. Individual lubricant of Sn-Ag-Cu or  $C_{60}$  provided a slight enhancement on the tribological performances of M50. This Sn-Ag-Cu exhibited excellent lubrication behavior in M50 under the loads of 2–12 N; nevertheless, its lubrication effect was basically lost under a high load of >12 N. In contrast to Sn-Ag-Cu, the  $C_{60}$  particles could afford M50 with superior lubricating ability at the loads of 12–18 N; nevertheless, its lubricating influence was unobvious below 12 N. It was noteworthy that, over a wide loads range 2–18 N, MSAC-C composites were proven to have outstanding tribological behaviors owing to the load-adaptive effect of mixed lubricant (Sn-Ag-Cu)- $C_{60}$ . Important tribological mechanism was further proposed. The  $C_{60}$  particles were distributed on the wear surface, and formed a film rich in (50Sn40Ag10Cu) (MSAC)/ $C_{60}$  on the MSAC-C wear surface;  $C_{60}$  was encapsulated in Sn-Ag-Cu. Such Sn-Ag-Cu spreading not only played a lubricating role but also contributed to the refinement of the encapsulated  $C_{60}$  particles, leading to an excellent lubrication effect (Figure 4(d)).

These abovementioned results provide convincing observations of composites reinforced by fullerenes. Interestingly, fullerenes showed enormous potential for friction-reduction and antiwear enhancement at current and future research works for a myriad of micro/macrotribology applications; this is attributed to the tiny ball bearings.

**3.2. Carbon Nanotubes.** Motivated by the 1D tubular structure, CNT has responded positively in improving the mechanical properties of materials for aerospace, automotive and biomedical applications [95–98]. The developments of these crucial fields, however, are further limited by friction and wear. Tribological potentials of CNTs make them promising candidates for the enhancements of bulk materials [99, 100]. Several discussions of CNTs in improving tribological behaviors of the bulk materials are conducted in this section.

Reasonable external conditions, such as CNT contents, applied loads, and working temperatures, are very attractive for the improvements of friction reduction and wear resistance properties [84, 101]. In our group's works, the effects of MWCNTs and Ag on TiAl-based composites under several loads and temperatures have been explored [84]. TiAl-substrated composite containing 4.0 wt%-Ag and 1.7 wt%-MWCNTs exhibited small friction coefficient and low wear rate at 13 N–450°C. Observations indicated Ag was enriched in the wear scar and adhered to the MWCNTs. A lubrication film containing Ag and MWCNT was obtained during friction, resulting in an outstanding tribological ability of the composite. However, high concentration of CNTs is an obstacle to the formation of lubricating film. The report of Lammini et al. [102] indicated that 10 wt%-MWCNTs difficultly protected tribofilm from the brittle fracture during wear, owing to the structural defects (e.g., agglomeration and porosity) of MWCNTs-reinforced 8 mol% yttria-stabilized zirconia (MWCNTs/8YSZ) composites. Adding 1 wt%-MWCNTs into the 8YSZ resulted in a significant

improvement in wear resistant, as compared with pure 8YSZ; this mainly attributed to the formation of a continuous tribofilm and the improvements in flexural strength, fracture toughness, and density. In another study [103], in contrast to pure AMMA, polyacrylonitrile-methylmethacrylate-CNTs (AMMA-1.5 wt% CNTs) composites exhibited smaller friction coefficient and higher wear resistance. CNT was uniformly dispersed in their matrixes during wear, which could serve as a medium, thereby preventing the direct contact of tribointerfaces.

Meanwhile, the aspect ratio (AR) of CNTs also dominates the friction and wear performances of the matrix materials [104]. The roles of high/low AR CNTs (HARC/LARC) on tribological behaviors of UHMWPE were reported [104]. If compared to neat UHMWPE, antiwear and antifriction abilities of the composites were significantly improved by ~530% and ~220% using HARC, respectively. It was remarkable that, HARC had the better enhancement effect compared with LARC; this was because a good interfacial bonding between the HARC and UHMWPE matrix was achieved, which increased the load-transferring ability from matrix to CNT.

Adding CNTs into AMMA-CNTs copolymer nanocomposites can induce potential enhancements for load-carrying capacity, antifriction, wear resistance, and thermal stability [104–106]. Figures 5(a) and 5(b) exhibit the typical SEM images of worn surfaces of pure AMMA and its composite. Figure 5(a) indicates that the wear surface of AMMA showed obvious plowed furrows. By contrast, the scuffing and adhesion of 1.5 wt% AMMA-CNTs composites were significantly reduced (Figure 5(b)) [105]. Schematic of the test configuration is displayed in Figure 5(c) [106]. The data are summarized in a direct way, average friction coefficient and the wear of the polymeric materials are plotted in Figure 5(d) and 5(f), which were organized by Yang et al. [84]. It was obvious that the wear showed a decreasing tendency with the lower friction coefficients and vice versa.

Influences of MWCNTs and GO on the tribological behaviors of UHMWPE were studied under water lubrication conditions [106]. GO/MWCNTs-reinforced composites exhibited a lower friction and higher wear resistance, in contrast to pure UHMWPE. Such improvement is mainly attributed to the synergistic lubrication of MWCNTs and GO. Surface coverage area of CNTs ( $R_{c/m}$ ), played a significant role in the wear resistance of epoxy matrix composites [99]. The wear rates of high  $R_{c/m}$  composites remained low during friction, which were ~3.2 times smaller than that of sample with  $R_{c/m} < 25\%$ , and 5.5 times lower than that of pure epoxy. Improvement in wear resistance was because CNTs were deformed and fragmented, thus exposing to sliding interface, which effectively reduced the wear.

Unique tribofilms of CNTs were induced in different operational conditions, such as loads and temperatures; these were responsible for significant enhancements in the tribological behaviors. The incorporation of CNTs and other nanomaterials improved the structure defects of CNTs (namely, agglomeration and porosity), thus resulting in the realization of superior antifriction and antiwear abilities.

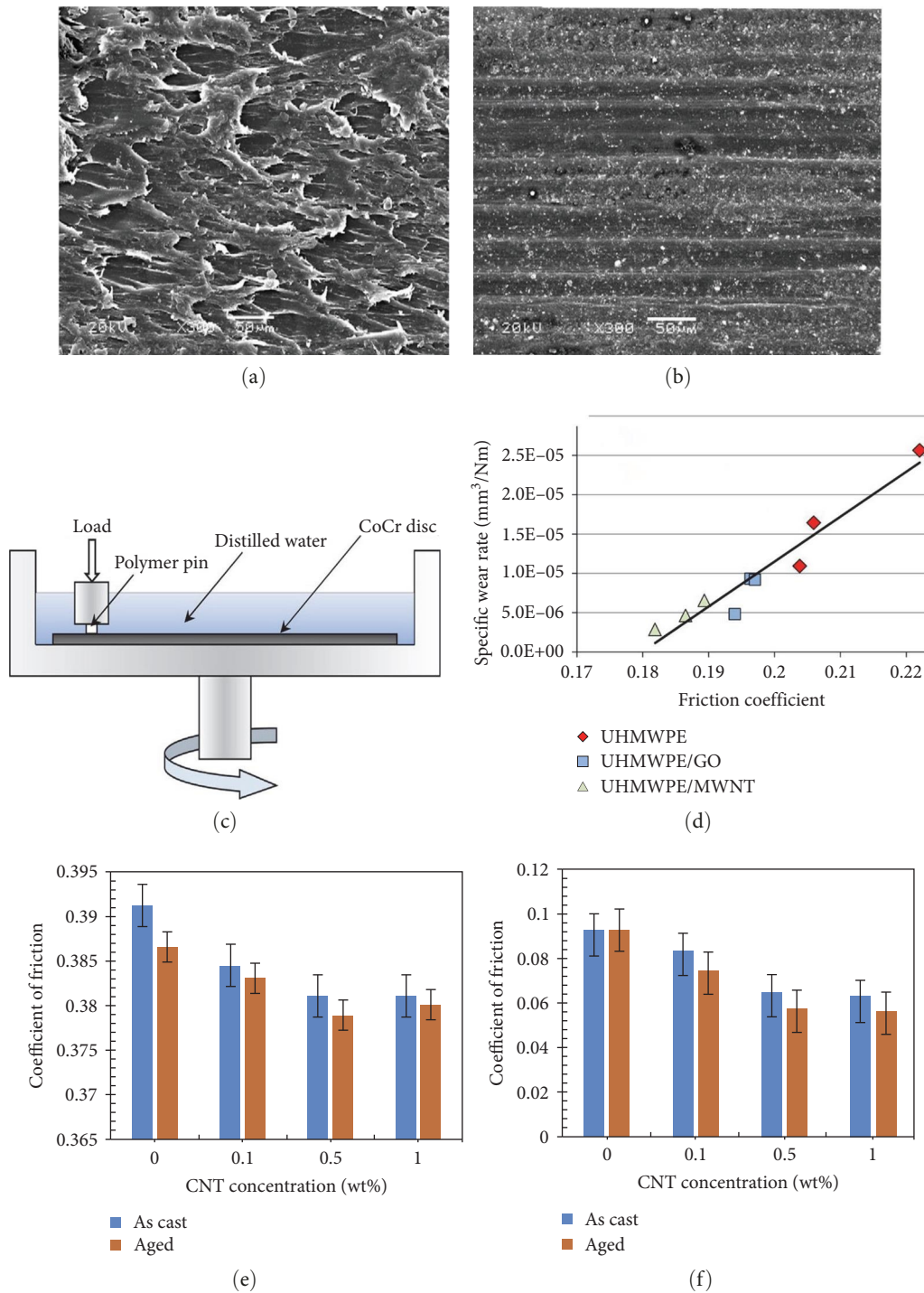


FIGURE 5: (a) Wear surface SEM images of polyacrylonitrile methyl methacrylate (AMMA) and (b) AMMA-CNTs with 1.5 wt%-CNT [105]; (c) schematic of test configuration; (d) specific wear rates vs. average friction coefficients [106]; mean friction coefficients (e) and wear rates (f) of TiAl substrate composite [84].

**3.3. Graphene.** Splendid mechanical and thermal characteristics of graphene have shown a huge potential for the expected improvements of tribological behaviors at harsh operating conditions, such as high temperatures, heavy loads, and high vacuum [107–109]. Moreover, its self-lubricating effects, tribofilm formation, and synergism with other components, etc. determine the tribological properties of bulk

material systems. Systematic discussions on tribological properties of the graphene-containing block materials are of great scientific significance and engineering value.

Reports of graphene-reinforced TiAl matrix composites have ensured that [110], the introduction of graphene decreased friction coefficients and wear rates. More specifically, the graphene was easy-to-shear and formed a

protective tribofilm on the wear interfaces, thereby enhancing the tribological behaviors of composites. Based on recent study, wear rate of the material was close with  $H/E$  ratio [85], the ratio of hardness  $H$  to elastic modulus  $E$  was widely acceptable in determining the limit of elastic surface contact, which was significant in wear resistance [111–113]. Liu et al. [112] prepared several graphene/Ni composites by using in situ powder metallurgy process. Due to the Zener pinning effect produced by graphene nanosheets, the grain growth of Ni matrix was inhibited with the increase of carbon source. The hardness and tribological properties of nickel matrix were greatly improved by graphene. The  $H/E$  ratio of the composite with 0.6 wt% carbon content was the highest, and the COF and wear resistance were 0.254 and  $4.385 \times 10^{-5} \text{ mm}^3/\text{Nm}$ , respectively. Compared with pure Ni, the friction coefficient and wear rate of a 0.6 wt% graphene/Ni composite were reduced by 3.02 and 3.44 folds, respectively. Addition of 0.6 wt% graphene led to an increase in the  $H/E$  ratio, therefore improving wear resistance ability.

Besides, synergism of the multiple elements is considered an attractive strategy to improve tribological properties [86, 114]. Study of Al/graphene/ $\text{ZrO}_2$  composites by Zhang et al. [86] showed that the self-lubricating properties of graphene had a positive effect on reducing the contact between the substrate and friction pair, thereby reduced friction. Nano- $\text{ZrO}_2$  particles improved the hardness and wear resistance of composites. Recently, there have been several reports on the suitability of graphene and  $\text{MoS}_2$  particles for various applications. The tribological properties of graphene and  $\text{MoS}_2$  as liquid–solid fillers in epoxy resin and dry media were studied. Compared with raw epoxy and binary epoxy composites, the addition of nanogenes in the epoxy- $\text{MoS}_2$  matrix reduced the influence of water on  $\text{MoS}_2$  and enhanced the intermolecular van der Waals forces due to synergistic effect of graphene and  $\text{MoS}_2$ . The alignment of nanogenes with  $\text{MoS}_2$  particles parallel to sliding direction facilitated the  $\text{MoS}_2$  lubrication. Epoxy/graphene/ $\text{MoS}_2$  exhibited the smallest COF and wear rate under selected conditions [114]. In addition, graphene could work in concert with natural nanofibers of large sizes, such as coconut shell fibers. Natural plant fiber could enhance the friction and wear properties of polymer biocomposites, which had a very important practical application value. However, it was still challenging to design the interface interaction between fiber and polymer matrix, which also determined the tribological properties of composites. The synergistic interaction of graphene and coconut shell fibers promoted the crystallization of polypropylene chain, resulting in high hardness. The prepared composites obtained high interfacial bonding interactions and exhibited lower friction coefficients and wear rates [115].

In summary, graphene has been shown to exhibit a honeycomb network of  $\text{sp}^2$ -bonded carbon atoms, which is responsible for its extraordinary in-plane mechanical strength. Aforementioned works enrich current research progress on bulk materials by involving graphene; a tribofilm was formed at the friction interface during wear, thus leading to the reduced frictional resistance and wear loss of material.

Thereby, this will open up the further possibilities for exploring novel graphene-containing bulk materials with potentials of low friction and good antiwear ability by controlling graphene contents and its surface functionalization.

**3.4. Nanodiamonds.** NDs inherit the unique properties of diamonds, such as high strength, high mobility of charge, good thermal conductivity, and low coefficient of thermal expansion, thus, exhibiting great potential for tailoring mechanical and tribological behaviors. Self-lubricating mechanism (polishing, rolling), tribofilm formation and altered wear mechanisms of NDs dominate the friction-reducing behavior and antiwear ability of composite systems. Poor dispersion of NDs remains an obstacle for the achievement of excellent tribological properties of composites. A strategy of surface modification was used to improve ND dispersion in Al alloy; NDs closely contacted with the matrix, resulting in the formation of reaction-free interfaces [116].

Huang et al. [117] prepared an ND-reinforced Fe matrix composite in hot-press sintering. A pearlite microstructure was formed due to the reaction between Fe and ND in the sintering. Presence of ND provided high hardness, compressive strength, and flexural strength. Concretely, adding 1 wt% ND increased the hardness by 51.5%, the compressive strength by 37.4%, and the flexural strength by 76.2%. At the same time, the unreacted ND particles were pressed and applied, forming a solid lubricant film, which was also one of the reasons for the decrease of COF. Therefore, the wear resistance and friction resistance of the alloy tended to increase with the increase of ND concentration. Meanwhile, the antiwear and friction resistant showed increasing tendency as the ND concentration increases.

For composites, the addition of well-dispersed homogeneous nanocarbons can effectively improve the mechanical and tribological properties, while the effect on the contact area varied with the addition concentration. As shown in Table 1, a summary of some nanoadditives in terms of friction coefficients and wear results under different conditions were listed. This shows that suitable carbon nanoadditives can effectively achieve wear reduction and antiwear enhancements.

## 4. Additives for Lubricants

Lubricants have been proven to be widely useable for controlling the friction and wear of contact parts, such as gears, bearings, and scrolls [122, 123]. Based on the constant evolution, oil viscosity and additive play the crucial roles in improving the triboperformances of lubricants. Nanoscaled additives in lubricants have been confirmed to exhibit better properties compared to traditional additives. This section discusses the latest progress on carbon nanoadditives for the enhancement of friction-reducing and antiwear abilities of lubricants.

**4.1. Fullerenes.** Researches on fullerenes have received huge interest in the field of tribology owing to their high electron mobility, availability for chemical modifications, and excellent ball-bearing effects [124–126]. This subsection will

TABLE 1: Tribological performances of CNTs-reinforced composite coatings.

Matrixes	Additives	Conditions	Contents	Friction coefficients, wear ( $\text{mm}^3/\text{Nm}$ )
Mg-1Al [92]	Fullerene	48 mm/s, 20 N	0.5 wt%	$\sim 0.4$ , $\sim 0.015$
		96 mm/s, 20 N		$\sim 0.385$ , $\sim 0.017$
Epoxy [118]	$C_{70}$	4 N	1 wt%	$\sim 0.234$ , $\sim 0.0126$
			3 wt%	$\sim 0.168$ , $\sim 0.0024$
Al 7075 [101]	CNTs	450 (rpm), 20 N	0.75 p	$8.8 \mu\text{m}/\text{min}$
Al [119]	MWCNT	450 (rpm), 60 N		$15.2 \mu\text{m}/\text{min}$
Epoxy [118]	MWCNTs	4 N	4.5 vol%	$0.042$ , $\sim 36.6$
			1 wt%	$\sim 0.171$ , $\sim 0.092$
CuO [120]	Graphene	1.1 GPa	3 wt%	$\sim 0.188$ , $\sim 0.032$
		2.0 GPa		$\sim 0.09$ , $\sim 0.0287$
Epoxy [73]	NDs	1,000 m, 10 N	0.25 wt%	$\sim 0.10$ , $\sim 0.0528$
			0.75 wt%	$\sim 0.38$ , $\sim 0.516$
Ti [121]	NDs	200 N	0.1 wt%	$\sim 0.22$ , $\sim 0.352$
			0.5 wt%	Wear $\sim 0.89\%$
				Wear $\sim 0.41\%$

orderly highlight and demonstrate recent advances of fullerenes for improving the friction reduction and material wear resistance performances of tribosystems.

In contrast to traditional lubricants, the fullerene-containing lubricants can achieve significant adjustments in friction-reduction and antiwear enhancement. Study of Lee et al. [127] showed that the friction coefficient of fullerene-reinforced refrigerating oil (0.02) was lower than that of pure oil (0.03). It was noteworthy that, an excellent dispersion and the formation of a tribofilm produced the positive influence in the lubricating performance. Different from aforementioned work of Lee et al. [127], Ku et al. [128] indicated that an enhanced load-bearing capacity of the oil by  $C_{60}$  was considered to be the direct reason for improvements of antifriction and antiwear abilities. Similarly, the addition of up to 0.5 wt%-fullerene soot achieved a decrease ( $\sim 30\%$ ) in friction force after tests [129]. This improvement in the ultimate load-bearing capacity of lubricating layer caused by employing fullerene was helpful in improving tribological behaviors of base oil.

In summary, fullerene  $C_{60}$  has achieved high dispersion and friction-film in oil that encourages the improvements in friction-reduction and antiwear abilities. Meanwhile, extra enhancement in load-bearing capacity promotes the applications under complex working conditions. Further explorations on the excellent modifications of fullerenes for reducing their agglomeration must be carried out.

**4.2. Carbon Nanotubes.** As the rapid development of industries, lubricants have been proven to be widely useable for reducing friction and wear. However, low friction and wear for lubricants are difficultly achieved in succession under severe operating conditions. Motivated by this, CNTs-reinforced lubricants are increasingly being regarded as advantageous reinforcements for improving tribological behaviors [130, 131]. Nevertheless, high concentrations' CNTs induce the agglomeration; thus, preventing CNT aggregation and creating homogeneous dispersion deserved more attentions [132, 133].

Moderate concentrations of MWCNTs have verified excellent dispersion stability and good compatibility with the base lubricant [3]. It was observed that the addition of 0.03 wt% MWCNTs led to a 6% friction reduction in engine. If compared to single enhancement, the synergism effects of multiple additives have an increasing trend for achieving good antifriction and antiwear properties [130]. The engine oil containing ZnO/MWCNTs was found to show better friction-reduction and antiwear capabilities than those of oil with ZnO or MWCNTs. When the friction pair was lubricated by oil with ZnO/MWCNTs, the additives were gradually deposited on the pits and grooves and penetrated into the contact interface, thus forming a protective film on the friction surface. The ZnO/MWCNTs composite in the base oil prevented the rough surface of the friction surface from contacting directly by increasing the thickness of oil film. Thus, the lubricating properties of base oil were significantly enhanced. Hard abrasive particles were significantly reduced and a smooth wear surface was obtained. Synergistic lubrication effect reduced the friction and wear of the contact surface.

Golchin et al. [106] reported the effects of GO/MWCNTs on tribological behaviors of lubricants. Adding 0.1 wt%-SWCNTs into polyalphaolefin base oil caused a reduction in friction coefficient under various contact pressures (0.83–1.42 GPa). As for the effect of MWCNTs on tribological characteristics of the same oil, it was found that the friction coefficient decreased to  $\sim 0.15$  upon the incorporation of 0.1 wt% MWCNTs at 0.83 GPa.

Typical preparation diagram of OMWCNTs and AMWCNTs, and the dispersibility of OMWCNTs in water and AMWCNTs in LP are displayed in Figure 6(a). Hydrophilic hydroxyl groups induced the better dispersion of OMWCNTs in water than MWCNTs [134]. MWCNTs had high van der Waals forces and high ARs, which were not easy to disperse uniformly in the ceramic matrix, and proper surface modification was required to overcome the agglomeration problem. To solve this problem, MWCNTs were acid

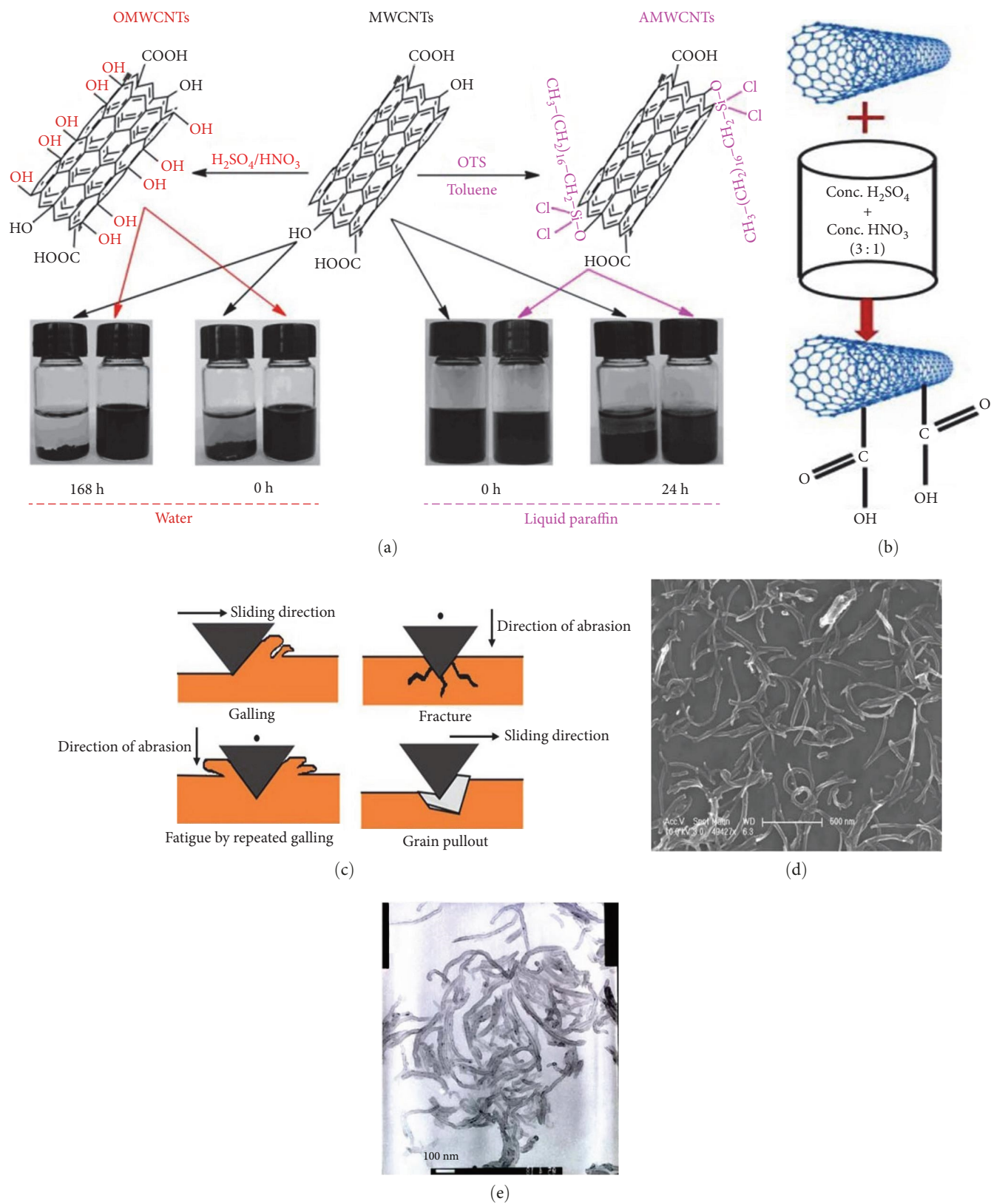


FIGURE 6: (a) Preparation schematic of OMWCNTs and AMWCNTs [134]; (b) process of acid functionalization of MWCNTs; (c) diagram of various wear mechanisms [135]; (d, e) SEM and TEM images of the oxidized MWCNTs [136].

functionalized with  $\text{H}_2\text{SO}_4$  and  $\text{HNO}_3$  in the ratio of 3 : 1. This functionalization process is shown in Figure 6(b). Schematic of the abrasion during wear is shown in Figure 6(c) [135]. SEM and TEM images of the oxidized and dispersed MWCNTs are shown in Figure 6(d) and 6(e). It observed that the oxidized MWCNTs were well-dispersed and mainly distributed in the form of isolated tubes [136]. The functionalization of CNTs by surfactants improved the water solubility of CNTs, resulting in uniform dispersion. The main principle of sodium dodecyl sulfate (SDS)-functionalized MWCNT additive to reduce the friction and wear of steel-steel sliding system was realized by chemical adsorption on the steel surface and filling the groove of the mating surface, and the dispersibility of MWCNTs in water also played an important role.

Liu et al. [131] fabricated functionalized MWCNTs reinforced bismaleimide resin lubricant. The tribological behavior of functionalized CNT-filled paraffin oil-lubricated bismaleimide resin was investigated by a friction and wear tester, and it was found that the addition of this functionalized MWCNTs at a concentration of 0.025 wt% had the best effect on reducing the friction coefficient. The topology of f-MWCNTs was not much different from that of original MWCNTs, which was beneficial to maintain the excellent mechanical properties of MWCNTs. This enabled them to generate high-quality isolation media. When f-MWCNTs were used as lubricant additives, the f-MWCNTs particles were trapped in the sliding interface of the interfacial patch, formed a tribofilm, prevented direct action on the contact surface, thereby dispersing high contact pressure and avoiding lubrication in pure oil invalid. The lubricants exhibited good improvements in antifriction and antiwear, owing to functionalized isolating effect and bearing structure off-MWCNTs. Similar to aforementioned study, Peng et al. [136] prepared another modified-MWCNTs by SDS for the same objectives. Since MWCNTs easily slide or roll between the two mating surfaces, the shear stress was very low and the friction coefficient was greatly reduced. During wear, well-dispersed MWCNTs were easily deposited in the valleys of two tribosurfaces, preventing the concave-convex contact and furrowing between two mating surfaces, thus greatly reduced wear. The chemical treatment of MWCNT surface had a significant effect on its lubricating properties, COF, and wear life. Moreover, SDS aqueous solution was not only a surfactant, but also a good dispersant. With the addition of SDS, the dispersibility of MWCNTs in water was further improved. During wear, SDS itself was adsorbed on the wear surface, thereby improving the antifriction and antiwear ability of the composite material. In short, the material damages were effectively resisted, meanwhile, the utilization of additives with functionalized MWCNTs resulted in an increase of friction resistance and the reduction of material loss.

Different additives can generate characteristic properties (namely, good dispersion stability and chemical stability) for improving friction and wear behaviors. In addition, surface functionalization of additives possibly produces new physical structures; this bearing capacity may be affected by their

inter-conversion, thus causing the lubricating ability to be improved well.

**4.3. Graphene.** Reports on the large-scale use of dispersed-nanoparticles have been proven in tribological characteristics of lubricant. The wear and friction behaviors on the plateau honed cylinder liner surface with graphene-added nanolubricant were investigated by Javeed et al. [137], after GO dispersed in diesel engine oil. Due to the accelerated wear during the initial run-in period, the contact area between the top and bottom specimens increased and resulted in a better force distribution between tribomating pairs. Because of the increased contact area, the contact pressure was reduced and the wear trend was almost stagnant. In this case, sheet-like multilayered GO entered the matched pairs and avoided metal contact under boundary lubrication conditions. It was further inferred that at high GO concentrations, a high wear effect was found. A small amount of GO nanoparticles provided a nanocarrying effect due to their entrapment between friction pairs. No excessive wear occurred in this case, resulting in an improved performance. Notably, low-concentration nanoparticles could provide good lubricity for the friction pair through the nanoloading effect. Conversely, higher nanomaterial concentrations led to excessive and accelerated wear, resulting in higher friction.

Aminated silica-modified GO (SAG) was fabricated, and several SAG aqueous dispersions with different mass percent were prepared with the help of ultrasonic mixing in deionized (DI) water; these specific methods are illustrated in Figure 7(a) [138]. Nano-SAG had good dispersibility, and combined the advantages of silica nanoparticles and GO nanosheets. In DI water and high contact pressure, the SAG resistance to abrasiveness was significantly improved. 3D topography images and 2D profiles of the wear tracks on the plate are shown in Figures 7(b) and 7(c). It can be found from the figure that after adding 0.5 wt% GO nanofluid to water, the wear rate was greatly reduced compared with pure water. In sharp contrast, the wear rate of 0.5 wt% GO nanofluid lubrication was one order of magnitude lower than that of pure water lubrication, and the wear trajectory of pure water lubrication was significantly deeper than that of nanofluid lubrication. Therefore, the enhanced lubrication of 0.5 wt% GO was confirmed by the shallower wear trajectory [139].

Further, Kinoshita et al. [140] produced water-based lubricants with GO monolayer sheets. With the addition of GO, the friction coefficient was proven to be  $\sim 0.05$  with a slight wear after 60,000 cycles. Such remarkable friction data was because GO adsorption occurred on the lubricated surfaces of both the ball and flat plate, acting the role as protective coatings.

In summary, friction and wear performances of graphene-reinforced lubricants mainly rely on the dispersion uniformity of graphene in the matrix and the formation of a tribofilm during friction. Modified graphene also provides an effective way for optimizing the friction and wear performances of lubricants, by constructing well-dispersed nanolubricants. Moreover, the almost impeccable interface

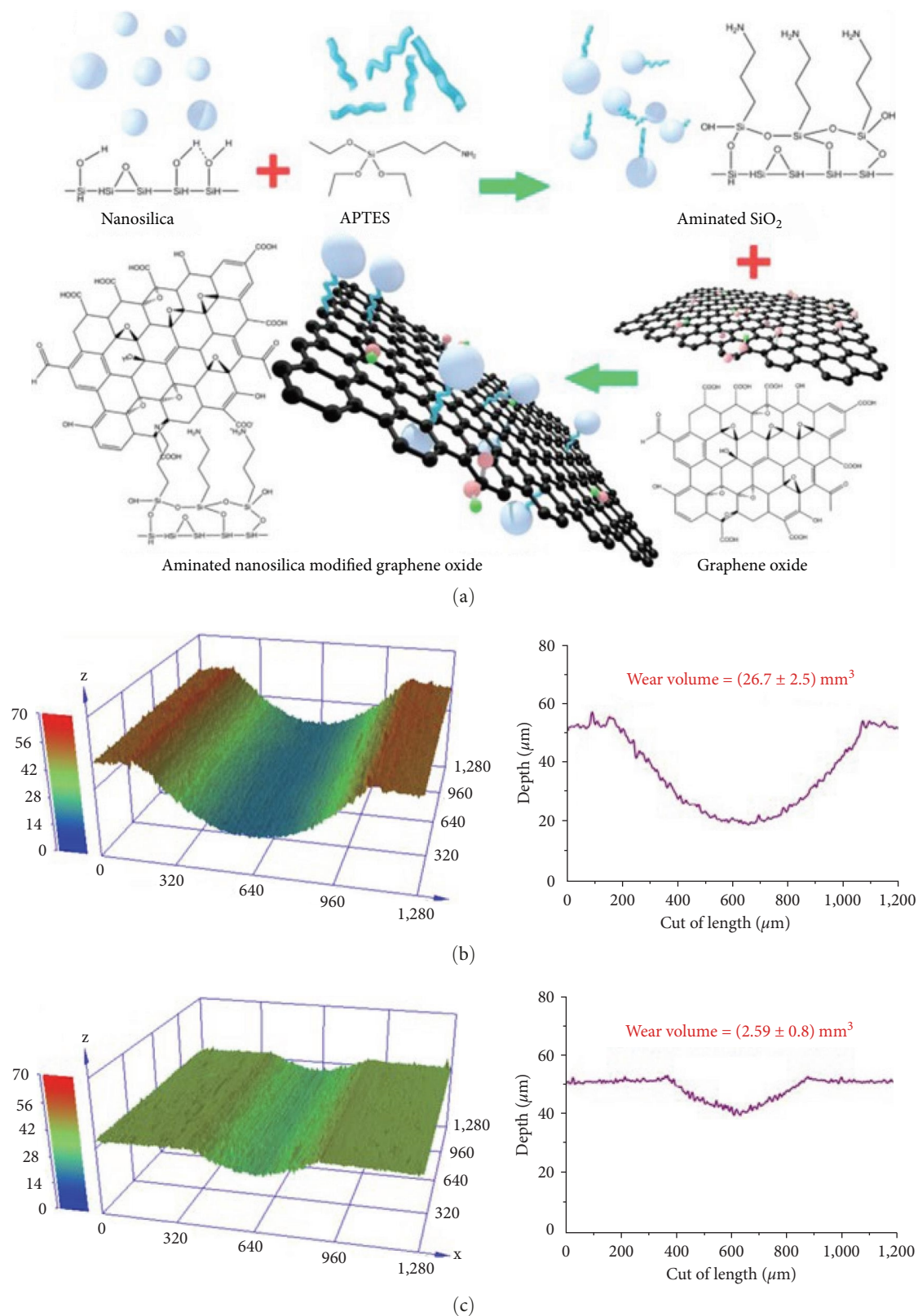


FIGURE 7: (a) Aminated silica-modified graphene oxide was prepared in showed schematic [138]; 3D topography images and 2D profiles across wear tracks for flat specimens after wear tests with (b) pure water; (c) 0.5 wt% GO nanofluids (3, 0.08 m/s, 30 min), the GO additives exhibit considerable enhancement in antiwear performances about  $26.7 \text{ mm}^3$  to  $2.59 \text{ mm}^3$  [139].

coverage on the relative slipping surface, via the utilization of graphene and GO has been obtained.

**4.4. Nanodiamonds.** NDs have demonstrated unique mechanical properties of partially rigid diamond cores, such as high hardness and good heat dissipation, with easily modified surfaces, which directly lead to the wear resistance of the material [141–143]. Several particular adhibitions on the utilization of NDs for lubricants have been widely studied, which are discussed in this section.

Tribological properties of nanopowder in aqueous suspension were studied in detail by molecular dynamics simulation [141]. Adding of NDs showed significant improvements in lubrication ability of water; the reductions in friction (70%) and wear (88%) were achieved. Based on the ethylene glycol lubrication, addition of 3.7 wt% NDs led to a reduction from 0.16 to 0.11 in friction coefficient, which was ascribed to the formation of an ND-mediated lubricating layer [144]. NDs-reinforced oil also significantly improved the antifriction and antiwear performance of the micro steel/copper interface [142]. Friction torque decreased by 0.08, which could be ascribed to the well-dispersed 0.2 wt% NDs, while the friction torque in pure oil was approximately three times higher than of reinforced one. Particularly, the wear volume of the oil with ND was lower than that without NDs.

Novel water-based lubricant containing GO and ND was reported [145]. Friction test confirmed a low friction coefficient of  $\sim 0.03$  for the prepared lubricant with 0.1 wt% GO and 0.5 wt% ND. GO was well dispersed in water and easily entered the contact area that protected the direct contact between friction pairs, thus reducing friction and wear. Due to the “ball bearing” effect, ND particles might roll between tribopairs during friction, converted the sliding friction into a combination of rolling friction and sliding friction, thereby achieved an improved tribological property. In addition, ND was adsorbed on the worn surface to form a tribofilm. Such tribofilm composed of NDs and an amorphous matrix of carbon, prevented the direct contact between tribosurfaces, helping in the improvement of frictional behavior of lubricant.

## 5. Superlubricity

Although lubricants can be used for improving tribological behaviors, ultimately it is the energy saved by a tribological system that is crucial [146–148]. Superlubricity can be divided into two forms, namely, nonproportional contact and disordered solid interface superlubrication. Researchers have proven the improvements of carbon nanomaterials in mentioned two superlubrication modes to be outstanding [149–151]. This section summarizes the studies on fullerenes, CNTs, graphene, and NDs for superlubricity.

**5.1. Fullerenes.** Superlubricity was an emerging research focus for realizing energy conservation and extending the lifetime of the mechanical components [152, 153]. So far, superlubricity with exceptionally low energy dissipation has been observed in experimental and simulation works at

both the micro-scale and macroscale under various friction conditions, in which the studied systems were mainly based on carbon materials.

Motivate by this, the onion-like carbon coating in lubricated system for incommensurate contact was explored by Gong et al. [154]. The coating not only was found to have superhigh elastic recovery (92%), but also exhibited ultralow friction coefficient of 0.01 and wear rate of about  $6.41 \times 10^{-18} \text{ m}^3 \text{ Nm}^{-1}$ . To further understood the positive effect of nanostructure evolution on superlubricity, the  $\text{Al}_2\text{O}_3$  spherical debris coated on the surface of the microgrid could be observed by HRTEM, and it was found that a large number of well-structured carbon onions (COs) composed the entire sample. The mutual sliding between atoms of COs and randomly arranged a-C atoms formed a disproportionate contact interface. Morphology and size distribution of the COs were similar to the volume distribution of COs/a-C films. During friction, the transferred fullerene particles formed many debris. Thus, rolling friction and disproportionate contact played an important role in the friction test. Interestingly, the COs achieved disproportionate contact and played a “molecular bearing” during friction, resulting in ultralow friction and wear rates.

The tribological behaviors of graphene/ $\text{C}_{60}$ /graphene with sandwich structure were investigated using MD simulations [155]. From the experimental results, it could be seen that the sandwich structure had good tribological properties, still had ultra-low friction less than 0.01 at the strength of 8 GPa, and did not depend on the surface roughness of the coating. The simulation data suggested that changes in the shape and deformation modes of  $\text{C}_{60}$  molecules were key to understanding the strength and friction of sandwich structures. The airtightly packaged  $\text{C}_{60}$  film retarded its plastic deformation by deforming the  $\text{C}_{60}$  molecules into oblate spheres through their ability to elastically support high-pressure loads. Overall, the graphene/ $\text{C}_{60}$ /graphene had excellent strength and tribological properties due to synergistic effect of graphene’s low friction coefficient and  $\text{C}_{60}$  molecule’s Nanometer properties, so this sandwich structure had many advantages in ultralow friction, strong, wear-resistant coatings, etc.

**5.2. Carbon Nanotubes.** CNT consists of coaxial cylindrical graphene layers with a high AR, which are ideal friction pairs for achieving superlubricity, because its surface is atomically smooth, and can form the highly incommensurate lattice [156, 157]. MWCNTs were honored as the smoothest bearings in geometry by theoretical modeling, and the interlayer friction was vanishingly small owing to the suppression of collective stick-slip motion in incommensurate tube pairs, similarly to superlubricity in graphite. Nevertheless, the CNTs we used frequently were not defect-free structure postulated in theoretical models. Various topological defects like vacancies, Stone–Wales defects, and adatoms inevitably introduced during MWCNT growth might lead to dissipation during intershell sliding in MWCNTs. These defects were introduced into the structure of the CNTs during their fabrication process, leading to the limitation of the superlubricity phenomenon in critical conditions.

DWCNTs have received a great deal of attention due to their great potential in the field of superlubricity. However, the various conditions, effects of point defect, size, intertube distance, occurred in fabrication process, which were the main impedes in realizing superlubricity. Li et al. [156] investigated the superlubricity behavior of a DWCNT comprising two tubes along the coaxial direction achieved by strain engineering by MD simulations. Influences of many factors were studied, including the misfit angle  $\varphi$ , magnitude of the strain  $\varepsilon$ , intertube distance  $\lambda_D$ , length  $L$  of the inner tube and degree of point defect  $\delta$ . Strain engineering presents the attractive potential to act in an effective and controllable way to realize the superlubricity of nanomaterials in practical applications.

Kis et al. [157] recorded the variations of MWCNTs in interlayer force under prolonged cyclic telescoping motion. However, the growth of CNTs inevitably resulted in the formation of defects, which modulated the van der Waals interaction between neighboring layers of MWCNTs, yet the motion exhibited ultralow friction. Moreover, the sliding nanotubes had a relative capacity to absorb induced damage when self-healing mechanism was triggered.

A remarkable noncommensurability structure of CNT made it possible to move relatively to each other along their common axis, which is the key factor for realizing superlubricity [158]. Based on MD simulation, the friction force was found to be closely contacted with CNT sliding velocity, interface contacted area, interface commensuration, and the temperature.

**5.3. Graphene.** Related tribological experiments of the graphene nanoscrolls, which were made up of graphite-like carbon (GLC) and fullerene-like-hydrogenated carbon (FLC) films reasonably indicated that the superlubricity could be achieved by forming graphene nanoscrolls coexisted at the sliding interface [151]. The formation of graphene nanoscrolls was caused by the different sliding-induced rehybridization rates and wear mechanisms between GLCs and FLCs under high loads. Under the same loads, GLC formed a perfect long-order graphene layer faster, so it will be worn first at high load, resulting in the direct contact between steel ball and the FLC and the formation of nanoparticle-like debris in the FLC [159, 160]. At 8 or 10 N, the graphene layer tended to wrap around the nanoparticles to form graphene nanoscrolls due to the spontaneous reduction of the nanoparticle surface energy.

When measuring points were >30 observed by a Raman microscope, at loads >8 N, Raman spectral distribution was found to appear frequently. This indicated a change in the number of graphene nanoscrolls [161, 162]. At the same time, the elastic recoil detection method determined that the hydrogen content of GLC and FLC was much lower than that required for the superlubricity of the disordered solid interface matrix demonstrated by the highly hydrogenated diamond-like carbon films ~40 at%. Through these data, it proved that the graphene nanoscrolls enhanced the macroscopic superlubricity (~0.005) and played a crucial role in achieving excellent antifriction performance of the friction pair.

Friction curve of the bilayer graphene sliding along the  $x$ -axis with a torsion angle of  $5^\circ$  is shown in Figure 8(a). Figure 8(b) records the potential energy of each atom in the initial state. Figure 8(c) illustrates the evolution of the Moiré pattern during the frictional change. The evolution velocity component of the Mohr pattern perpendicular to the direction of movement of the graphene layer during the frictional change was much larger than the evolution velocity component parallel to the direction of movement; this Mohr stripe moved forward in only half the period length ( $L_{\text{moiré}}$ ) of Moiré stripe parallel to the direction of movement. The change of friction was closely related to the evolution of Mohr stripe [163].

Synergistic lubrication of pristine graphene, fluorinated graphene, and GO coatings combined with glycerol was investigated [164]. Aqueous glycerol solution was added between  $\text{Si}_3\text{N}_4$  ball and graphene coating (Figure 8(d)), and then the macroscopic friction test was to examine the lubrication ability of glycerol combined with graphene coating (Figure 8(e)). Lubrication mechanism was shown in Figure 8(f). During grinding, graphene was adsorbed on the wear trajectory of a  $\text{SiO}_2$  substrate and transferred to  $\text{Si}_3\text{N}_4$  spheres, thereby achieving a boundary lubrication/graphene interface.

**5.4. Nanodiamonds.** Due to its outstanding tribological performance in friction interface, ND has been developed as another lubricity candidate used in potential applications to enable even superlubricity (friction coefficient lower than 0.01) at the sliding interface of moving mechanical-components. Chen et al. [165] reported the synergy of NDs and glycerol colloidal solution to achieve superlubricity at steel ball and disk. Composite solution caused considerable achievement in the superlubricity after a running-in period that was ascribed to the presence of NDs; the friction coefficient was 0.006 and the wear loss was less than pure one. Colloidal solution containing 0.01 wt% NDs led to a 32.5% reduction in the wear scar diameter and a 119.3% increase in the contact pressure between the rubbing surfaces. Ultralow friction coefficient was the result of hydrodynamic effects and hydrogen bond layers. The reduced wear was caused by the rolling effect of ND. As the mechanism of this novel liquid superlubrication system was revealed, it would be a great work to discover more superlubricity systems based on this mechanism. It was considered that regardless of the material of nanoparticles, as long as the surface of nanoparticles was hydrophilic or rich in hydrogen bonds, the nanoparticles could achieve superlubricity.

Where, wear scar was regarded as the Hertz elastic deformation of an imaginary ball, which was bigger than the real ball, under the original load. The radius of the imaginary ball could be calculated by Formula (3):

$$R^* = R \left( \frac{a^*}{a} \right)^3, \quad (3)$$

where  $R^*$  was the radius of the imaginary ball, and  $a$  was the radius of the wear scar on the ball. The Hamrock–Dowson

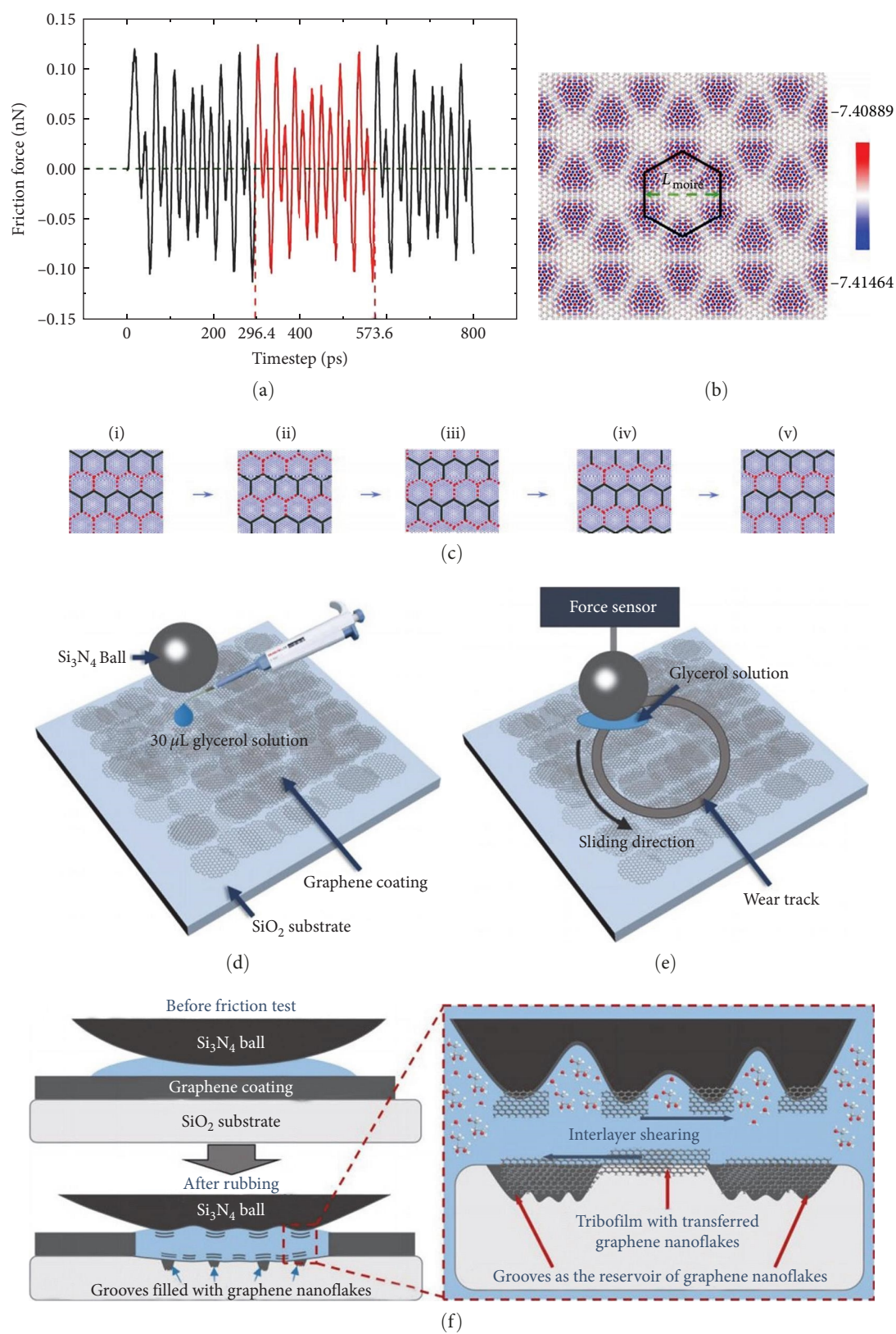


FIGURE 8: Evolution of Moiré patterns during interlayer sliding of bilayer graphene [163]. Schematic of the experimental procedure [164].

theory was applicable to an imaginary ball, and the minimum film thickness could be calculated by the following Formula (4):

$$H_{\min} = 3.63 \left( \frac{U^{0.68} G^{0.49}}{W^{0.073}} \right) (1 - e^{-0.26K}), \quad (4)$$

where  $H_{\min} = h_{\min}/R^*$ ,  $U = \eta V/E'R^*$ ,  $G = \alpha E'$ ,  $W = F/E'R^{*2}$ ,  $h_{\min}$  was the minimum film thickness,  $\eta$  was the bulk viscosity of lubricating solution,  $V$  was the averaged linear velocity of the ball and the disk,  $E'$  was the effective elastic modulus,  $F$  was the normal load,  $\alpha$  ( $\approx 5 \text{ GPa}^{-1}$  [166]) was the viscosity-pressure coefficient and  $k$  ( $\approx 1$ ) was the ellipticity parameter. According to the ratio of theoretical minimum film thickness to the combined surface roughness, the lubrication state was determined using Formula (5) [167]:

$$\lambda = \frac{h_{\min}}{\sigma} = \sqrt{h_{\min}/(\sigma_1^2 + \sigma_2^2)}, \quad (5)$$

where  $\sigma_1$  and  $\sigma_2$  were the roughness of the opposite rubbing surfaces after the lubrication tests, and  $\sigma$  was the combined surface roughness. For example, the calculated  $\lambda = 2.36$  and  $\lambda$  was less than 3, indicating that superlubricity was in the state of mixed lubrication.

## 6. Conclusions and Outlooks

Achieving low friction and high wear resistant is particularly critical for energy conservation. This review highlights recent developments and achievements regarding the large-scaled use of carbon nanomaterials for superior performances' tribomaterials (i.e., coatings, bulk composites, and compound nanolubricants) and superlubric states under nano/micro and macroscales. Numerous investigators have extensively demonstrated that an explosive progress in the forms of coatings, bulk materials, lubricants, and superlubricity for tribology has been achieved in carbon nanomaterials. Meanwhile, it is also verified that carbon nanomaterials exhibit superior tribological behaviors with underlying tribological mechanisms deriving from their multiple-type structures, excellent physical/chemical properties, high specific surface areas, etc. These achievements are relatively critical for the improvements of working efficiency, service life, and usage precision of mechanical systems, and provide versatile aisles in stimulating more new and complex friction applications.

Fullerenes and NDs own spherical shapes as well as high chemical stability, and have been shown to exhibit good lubricating properties, stable load-bearing abilities, and useful polishing effects. Meanwhile, due to its nontoxicity and biocompatibility, ND has a good prospect in biomedical applications, such as artificial joints. Owing to CNTs' linear structures, they are prone to providing a "bridging effect" to strengthen the interfacial bonding between them and substrates, that enabled the mechanical strength, toughness, and load-carrying capacity of matrix material to be significantly improved, thereby achieving low friction and wear. Furthermore, CNTs can be broken and crushed to form a

frictional film with low shear force during friction, reducing direct contact of tribosurfaces that provided low friction and small wear damage. With respect to graphene, in addition to the inherent weak van der Waals interactions between its layers, the exceptional thermal conductivity and the generation of a tribofilm are also beneficial to decrease the tribo-contacting area between two surfaces under limited load conditions, thus attaining an ideal tribological reinforcement for the composites. In addition, graphene can also impart a huge potential to enhance heat transfer and microstructural uniformity, because of its lamellar structure and thermal conductivity. Overall, these carbon nanomaterials play the important roles in the development of coatings, bulk self-lubricating composites, superlubricity, etc.

Although carbon nanomaterials have good potential for commercial application, there are still many challenges in related research. For fullerene molecule  $C_{120}$  with an optimal energy structure found by efficient computational ways [168], its tribological and adsorption properties are currently unknown; thus, studying them has become the main research subject of future research. Compared to traditional materials, carbon nanomaterials inevitably exist the defects and contamination, that weaken their friction-reducing and wear-resistant performances. It is noteworthy that these adverse effects can be improved by designing new preparation methods or rational surface microstructures. For example, the lubricity of graphene is susceptible to external interference, which can be compensated by the useful combination of graphene and other reinforcing materials. Finding efficient ways to break the gap between nanoscale and macroscale behavior has been discussed for decades. In this context, the use of graphene bulk materials and realization of superlubricity have been comprehensively studied, enabling advanced engineering applications ranging from surface engineering to large-scale manufacturing.

The foreseeable future of carbon nanomaterials in achieving huge tribological contributions, such as splendid antifriction and antiwear capacities, is coming. It is hoped that this work will provide more possibilities to realize relatively low friction, high wear resistance, or superlubrication state in the carbon nanomaterials-reinforced material systems such as copper coins and mechanical components. Moreover, the more in-depth explorations on carbon nanomaterials must be conducted, that are needed to obtain valuable discoveries for stimulating the commercial applications.

## Conflicts of Interest

The authors declare that they have no conflicts of interest.

## Acknowledgments

This study is supported by the Scientific Cultivation Foundation of Anyang Institute of Technology (YPY2021013); Project for Science and Technology Plan of Henan Province (212102210111, 212102210445); Key Training Project of Young Teacher of Henan province (2021GGJS149); Sichuan Provincial Key Lab of Process Equipment and Control

(GK201901). The authors are thankful for the special funding and equipment support of the visiting professor at the School of Materials Science and Engineering (4001-40734). The authors appreciate Nanjing XFNANO Materials Tech Co., Ltd for their kind assistance.

## References

- [1] A. Kotia, K. Chowdary, I. Srivastava, S. K. Ghosh, and M. K. A. Ali, "Carbon nanomaterials as friction modifiers in automotive engines: recent progress and perspectives," *Journal of Molecular Liquids*, vol. 310, Article ID 113200, 2020.
- [2] X. Li, X. Xu, Y. Zhou, K. R. Lee, and A. Wang, "Insights into friction dependence of carbon nanoparticles as oil-based lubricant additive at amorphous carbon interface," *Carbon*, vol. 150, pp. 465–474, 2019.
- [3] J. Kałużny, M. Waligórski, G. M. Szymański et al., "Reducing friction and engine vibrations with trace amounts of carbon nanotubes in the lubricating oil," *Tribology International*, vol. 151, Article ID 106484, 2020.
- [4] K. Yang, F. Zhang, Y. Chen, H. Zhang, B. Xiong, and H. Chen, "Recent progress on carbon-based composites in multidimensional applications," *Composites Part A: Applied Science and Manufacturing*, vol. 157, Article ID 106906, 2022.
- [5] D. Berman, S. A. Deshmukh, S. K. R. S. Sankaranarayanan, A. Erdemir, and A. V. Sumant, "Macroscale superlubricity enabled by graphene nanoscroll formation," *Science*, vol. 348, no. 6239, pp. 1118–1122, 2015.
- [6] F. Zhang, K. Yang, G. Liu et al., "Recent advances on graphene: synthesis, properties and applications," *Composites Part A: Applied Science and Manufacturing*, vol. 160, Article ID 107051, 2022.
- [7] H. Tang, J. Sun, J. He, and P. Wu, "Research progress of interface conditions and tribological reactions: a review," *Journal of Industrial and Engineering Chemistry*, vol. 94, pp. 105–121, 2021.
- [8] W. Wu, J. Liu, Z. Li et al., "Surface-functionalized nanoMOFs in oil for friction and wear reduction and antioxidation," *Chemical Engineering Journal*, vol. 410, Article ID 128306, 2021.
- [9] M. Prieske, H. Hasselbruch, A. Mehner, and F. Vollertsen, "Friction and wear performance of different carbon coatings for use in dry aluminium forming processes," *Surface and Coatings Technology*, vol. 357, pp. 1048–1059, 2019.
- [10] W. Zhao and F. Duan, "Friction properties of carbon nanoparticles (nanodiamond and nanoscroll) confined between DLC and a-SiO<sub>2</sub> surfaces," *Tribology International*, vol. 145, Article ID 106153, 2020.
- [11] C.-S. Chang, K.-H. Hou, M.-D. Ger, C.-K. Chung, and J.-F. Lin, "Effects of annealing temperature on microstructure, surface roughness, mechanical and tribological properties of Ni-P and Ni-P/SiC films," *Surface and Coatings Technology*, vol. 288, pp. 135–143, 2016.
- [12] B. Da, G. Yongxin, A. T. Vasu, L. Yaxuan, Z. Yongwu, and W. Yongguang, "Influence of GO-Al<sub>2</sub>O<sub>3</sub> hybrid material on the tribological behavior of chemically bonded ceramic coating," *Ceramics International*, vol. 46, no. 14, pp. 23027–23034, 2020.
- [13] B. Da, X. Rongli, G. Yongxin et al., "Tribological behavior of graphene reinforced chemically bonded ceramic coatings," *Ceramics International*, vol. 46, no. 4, pp. 4526–4531, 2020.
- [14] C. S. Richard, J. Lu, G. Bérannger, and F. Decomps, "Study of Cr<sub>2</sub>O<sub>3</sub> coatings part II: adhesion to a cast-iron substrate," *Journal of Thermal Spray Technology*, vol. 4, pp. 347–352, 1995.
- [15] J. Chen and S. J. Bull, "Modelling the limits of coating toughness in brittle coated systems," *Thin Solid Films*, vol. 517, no. 9, pp. 2945–2952, 2009.
- [16] P. Bagde, S. Mehar, S. G. Sapate, and A. Rathod, "Effect of graphite addition on tribological behaviour of plasma sprayed Cr<sub>2</sub>O<sub>3</sub>-TiO<sub>2</sub> coating," *Materials Today: Proceedings*, vol. 56, Part 4, pp. 2365–2370, 2022.
- [17] J. Zhang, S. Yang, Z. Chen, M. Wyszomirska, J. Zhao, and Z. Jiang, "Microstructure and tribological behaviour of alumina composites reinforced with SiC-graphene core-shell nanoparticles," *Tribology International*, vol. 131, pp. 94–101, 2019.
- [18] P.-R. Wu, Y.-C. Kong, Z.-S. Ma et al., "Preparation and tribological properties of novel zinc borate/MoS<sub>2</sub> nanocomposites in grease," *Journal of Alloys and Compounds*, vol. 740, pp. 823–829, 2018.
- [19] Z. Guan, P. Zhang, V. Florian et al., "Preparation and tribological behaviors of magnesium silicate hydroxide-MoS<sub>2</sub> nanoparticles as lubricant additive," *Wear*, vol. 492–493, Article ID 204237, 2022.
- [20] G. Tang, F. Su, X. Xu, and P. K. Chu, "2D black phosphorus dotted with silver nanoparticles: an excellent lubricant additive for tribological applications," *Chemical Engineering Journal*, vol. 392, Article ID 123631, 2020.
- [21] X. Chen and J. Li, "Superlubricity of carbon nanostructures," *Carbon*, vol. 158, pp. 1–23, 2020.
- [22] W. Ma, Z. Gong, K. Gao, L. Qiang, J. Zhang, and S. Yu, "Superlubricity achieved by carbon quantum dots in ionic liquid," *Materials Letters*, vol. 195, pp. 220–223, 2017.
- [23] L. Li, M. Ding, B. Lin, B. Zhang, Y. Zhang, and T. Sui, "Influence of silica nanoparticles on running-in performance of aqueous lubricated Si<sub>3</sub>N<sub>4</sub> ceramics," *Tribology International*, vol. 159, Article ID 106968, 2021.
- [24] R. Tonk, "The challenges and benefits of using carbon nano-tubes as friction modifier lubricant additives," *Materials Today: Proceedings*, vol. 37, Part 2, pp. 3275–3278, 2021.
- [25] A. K. Singh, N. Sinha, and A. P. S. Chauhan, "Frictional properties of dry multiwall carbon nanotubes (MWCNTs) nanoparticles," *Materials Today: Proceedings*, vol. 28, Part 1, pp. 266–268, 2020.
- [26] H. Song, J. Chen, N. Jiang, L. Ji, and J. Chen, "Low friction and wear properties of carbon nanomaterials in high vacuum environment," *Tribology International*, vol. 143, Article ID 106058, 2020.
- [27] I. Ali, A. A. Basheer, A. Kucherova et al., "Advances in carbon nanomaterials as lubricants modifiers," *Journal of Molecular Liquids*, vol. 279, pp. 251–266, 2019.
- [28] D. Liu, W. Zhao, S. Liu, Q. Cen, and Q. Xue, "Comparative tribological and corrosion resistance properties of epoxy composite coatings reinforced with functionalized fullerene C60 and graphene," *Surface and Coatings Technology*, vol. 286, pp. 354–364, 2016.
- [29] M. E. Turan, Y. Sun, and Y. Akgul, "Improved wear properties of magnesium matrix composite with the addition of fullerene using semi powder metallurgy," *Fullerene Nanotubes and Carbon Nanostructures*, vol. 26, no. 2, pp. 130–136, 2018.
- [30] M. Selvaraj, A. Hai, F. Banat, and M. A. Haija, "Application and prospects of carbon nanostructured materials in water treatment: a review," *Journal of Water Process Engineering*, vol. 33, Article ID 100996, 2020.

- [31] E. A. Eid and M. Ragab, "Effect of individual and hybrid additions of  $\text{Al}_2\text{O}_3$  NP and CNTs on the mechanical strengthening of aluminum-bronze alloy," *SN Applied Sciences*, vol. 2, Article ID 186, 2020.
- [32] H. Li, R. Papadakis, S. H. M. Jafri et al., "Superior adhesion of graphene nanoscrolls," *Communications Physics*, vol. 1, Article ID 44, 2018.
- [33] K. Babaei, A. Fattah-Alhosseini, and M. Molaei, "The effects of carbon-based additives on corrosion and wear properties of plasma electrolytic oxidation (PEO) coatings applied on Aluminum and its alloys: a review," *Surfaces and Interfaces*, vol. 21, Article ID 100677, 2020.
- [34] L. Zhou, T. B. Yuan, X. S. Yang et al., "Micro-scale prediction of effective thermal conductivity of CNT/Al composites by finite element method," *International Journal of Thermal Sciences*, vol. 171, Article ID 107206, 2022.
- [35] W. A. Shah, X. Luo, B. I. Rabiou, B. Huang, and Y. Q. Yang, "Toughness enhancement and thermal properties of graphene-CNTs reinforced  $\text{Al}_2\text{O}_3$  ceramic hybrid nanocomposites," *Chemical Physics Letters*, vol. 781, Article ID 138978, 2021.
- [36] L. Xiang, Q. Shen, Y. Zhang, W. Bai, and C. Nie, "One-step electrodeposited Ni-graphene composite coating with excellent tribological properties," *Surface and Coatings Technology*, vol. 373, pp. 38–46, 2019.
- [37] M. Bilal, H. Cheng, R. B. González-González, R. Parra-Saldívar, and H. M. N. Iqbal, "Bio-applications and biotechnological applications of nanodiamonds," *Journal of Materials Research and Technology*, vol. 15, pp. 6175–6189, 2021.
- [38] J.-X. Qin, X.-G. Yang, C.-F. Lv et al., "Nanodiamonds: synthesis, properties, and applications in nanomedicine," *Materials and Design*, vol. 210, Article ID 110091, 2021.
- [39] P. Y. M. Yew, D. D. Zhu, Q. Y. Lin et al., "Synergistic UV protection effects of the lignin nanodiamond complex," *Materials Today Chemistry*, vol. 22, Article ID 100574, 2021.
- [40] S. Adorinni, P. Rozhin, and S. Marchesan, "Smart hydrogels meet carbon nanomaterials for new frontiers in medicine," *Biomedicines*, vol. 9, no. 5, Article ID 570, 2021.
- [41] Z. Khorsandi, M. Borjian-Boroujeni, R. Yekani, and R. S. Varma, "Carbon nanomaterials with chitosan: a winning combination for drug delivery systems," *Journal of Drug Delivery Science and Technology*, vol. 66, Article ID 102847, 2021.
- [42] A. Fattah-Alhosseini and R. Chaharmahali, "Enhancing corrosion and wear performance of PEO coatings on Mg alloys using graphene and graphene oxide additions: a review," *FlatChem*, vol. 27, no. 6, Article ID 100241, 2021.
- [43] R. Taheri, M. Jalali, A. Al-Yaseri, and G. Yabesh, "Improving TC drill bit's efficiency and resistance to wear by graphene coating," *Petroleum Research*, Available online 22 December 2021.
- [44] X. Liu, M. Xiao, M. Liu, Z. Qiu, and D. Zeng, "Preparation and enhanced wear resistance of HVAF-sprayed Fe-TiB<sub>2</sub> cermet coating reinforced by carbon nanotubes," *Surface and Coatings Technology*, vol. 408, Article ID 126860, 2021.
- [45] Y.-R. Dong, W.-C. Sun, X.-J. Liu et al., "Effect of CNTs concentration on the microstructure and friction behavior of Ni-GO-CNTs composite coatings," *Surface and Coatings Technology*, vol. 359, pp. 141–149, 2019.
- [46] O. V. Penkov, V. E. Pukha, E. N. Zubarev, S.-S. Yoo, and D.-E. Kim, "Tribological properties of nanostructured DLC coatings deposited by C<sub>60</sub> ion beam," *Tribology International*, vol. 60, pp. 127–135, 2013.
- [47] J. Pu, Y. Mo, S. Wan, and L. Wang, "Fabrication of novel graphene-fullerene hybrid lubricating films based on self-assembly for MEMS applications," *Chemical Communications*, vol. 50, no. 4, pp. 469–471, 2014.
- [48] B. Chen, X. Li, Y. Jia et al., "Fabrication of ternary hybrid of carbon nanotubes/graphene oxide/MoS<sub>2</sub> and its enhancement on the tribological properties of epoxy composite coatings," *Composites Part A: Applied Science and Manufacturing*, vol. 115, pp. 157–165, 2018.
- [49] H. D. Lee, O. V. Penkov, and D. E. Kim, "Tribological behavior of dual-layer electroless-plated Ag-carbon nanotube coatings," *Thin Solid Films*, vol. 534, pp. 410–416, 2013.
- [50] I. Ahmad, A. Kennedy, and Y. Q. Zhu, "Wear resistant properties of multi-walled carbon nanotubes reinforced  $\text{Al}_2\text{O}_3$  nanocomposites," *Wear*, vol. 269, no. 1–2, pp. 71–78, 2010.
- [51] M. A. Samad and S. K. Sinha, "Mechanical, thermal and tribological characterization of a UHMWPE film reinforced with carbon nanotubes coated on steel," *Tribology International*, vol. 44, no. 12, pp. 1932–1941, 2011.
- [52] P. Tripathi, P. K. Katiyar, J. Ramkumar, and K. Balani, "Synergistic role of carbon nanotube and yttria stabilised zirconia reinforcement on wear and corrosion resistance of Cr-based nano-composite coatings," *Surface and Coatings Technology*, vol. 385, Article ID 125381, 2020.
- [53] M. A. Samad and S. K. Sinha, "Dry sliding and boundary lubrication performance of a UHMWPE/CNTs nanocomposite coating on steel substrates at elevated temperatures," *Wear*, vol. 270, no. 5–6, pp. 395–402, 2011.
- [54] S. Zhou, T. Xu, C. Hu, H. Wu, H. Liu, and X. Ma, "Utilizing carbon nanotubes in ceramic particle reinforced MMC coatings deposited by laser cladding with Inconel 625 wire," *Journal of Materials Research and Technology*, vol. 13, pp. 2026–2042, 2021.
- [55] J. Umeda, B. Fugetsu, E. Nishida, H. Miyaji, and K. Kondoh, "Friction behavior of network-structured CNT coating on pure titanium plate," *Applied Surface Science*, vol. 357, Part A, pp. 721–727, 2015.
- [56] G. Hatipoglu, M. Kartal, M. Uysal, T. Cetinkaya, and H. Akbulut, "The effect of sliding speed on the wear behavior of pulse electro Co-deposited Ni/MWCNT nanocomposite coatings," *Tribology International*, vol. 98, pp. 59–73, 2016.
- [57] A. Mura, F. Adamo, H. Wang, W. S. Leong, X. Ji, and J. Kong, "Investigation about tribological behavior of ABS and PC-ABS polymers coated with graphene," *Tribology International*, vol. 134, pp. 335–340, 2019.
- [58] B. S. Rajan, M. A. S. Bala, and A. B. M. A. Noorani, "Tribological performance of graphene/graphite filled phenolic composites-a comparative study," *Composites Communications*, vol. 15, pp. 34–39, 2019.
- [59] J. A. Puértolas, M. Castro, J. A. Morris, R. Ríos, and A. Ansón-Casaos, "Tribological and mechanical properties of graphene nanoplatelet/PEEK composites," *Carbon*, vol. 141, pp. 107–122, 2019.
- [60] O. L. Luévano-Cabrales, M. Alvarez-Vera, H. M. Hdz-García et al., "Effect of graphene oxide on wear resistance of polyester resin electrostatically deposited on steel sheets," *Wear*, vol. 426–427, Part A, pp. 296–301, 2019.
- [61] A. C. Ferrari and D. M. Basko, "Raman spectroscopy as a versatile tool for studying the properties of graphene," *Nature Nanotechnology*, vol. 8, pp. 235–246, 2013.

- [62] F. Wählich, J. Hoth, C. Held, T. Seyller, and R. Bennewitz, "Friction and atomic-layer-scale wear of graphitic lubricants on SiC0001 in dry sliding," *Wear*, vol. 300, no. 1–2, pp. 78–81, 2013.
- [63] A. L. Kitt, Z. Qi, S. Rémi, H. S. Park, A. K. Swan, and B. B. Goldberg, "How graphene slides: measurement and theory of strain-dependent frictional forces between graphene and SiO<sub>2</sub>," *Nano Letters*, vol. 13, no. 6, pp. 2605–2610, 2013.
- [64] K. Tripathi, G. Gyawali, and S. W. Lee, "Graphene coating via chemical vapor deposition for improving friction and wear of gray cast iron at interfaces," *ACS Applied Materials and Interfaces*, vol. 9, no. 37, pp. 32336–32351, 2017.
- [65] S. Singh, P. Verma, R. K. Gautam, and R. Tyagi, "Effect of counterface materials on friction and wear of graphene-coated steel under dry sliding contact," *Materials Today: Proceedings*, vol. 47, Part 19, pp. 6660–6663, 2021.
- [66] C. Lee, Q. Li, W. B. Kalb et al., "Frictional characteristics of atomically thin sheets," *Science*, vol. 328, no. 5974, pp. 76–80, 2010.
- [67] T. Filleter, J. L. McChesney, A. Bostwick et al., "Friction and dissipation in epitaxial graphene films," *Physical Review Letters*, vol. 102, no. 8, Article ID 086102, 2009.
- [68] S. Li, X. Dong, and Hanshan, "Improving the macro-scale tribology of monolayer graphene oxide coating on stainless steel by a silane bonding layer," *Materials Letters*, vol. 209, pp. 15–18, 2017.
- [69] M. Sadeghi, M. Kharaziha, and H. R. Salimijazi, "Double layer graphene oxide-PVP coatings on the textured Ti<sub>6</sub>Al<sub>4</sub>V for improvement of frictional and biological behavior," *Surface and Coatings Technology*, vol. 374, pp. 656–665, 2019.
- [70] J. Zhao, Y. He, Y. Wang, W. Wang, L. Yan, and J. Luo, "An investigation on the tribological properties of multilayer graphene and MoS<sub>2</sub> nanosheets as additives used in hydraulic applications," *Tribology International*, vol. 97, pp. 14–20, 2016.
- [71] H.-J. Kim and D.-E. Kim, "Water lubrication of stainless steel using reduced graphene oxide coating," *Scientific Reports*, vol. 5, Article ID 17034, 2015.
- [72] Y. Liu, D.-G. Shin, S. Xu, C.-L. Kim, and D.-E. Kim, "Understanding of the lubrication mechanism of reduced graphene oxide coating via dual in-situ monitoring of the chemical and topographic structural evolution," *Carbon*, vol. 173, pp. 941–952, 2021.
- [73] H. Aghamohammadi, A. Heidarpour, R. Jamshidi, and O. Bayat, "Tribological behavior of epoxy composites filled with nanodiamond and Ti<sub>3</sub>AlC<sub>2</sub>-TiC particles: a comparative study," *Ceramics International*, vol. 45, no. 7, Part A, pp. 9106–9113, 2019.
- [74] X. Chen, B. Zhang, Y. Gong, P. Zhou, and H. Li, "Mechanical properties of nanodiamond-reinforced hydroxyapatite composite coatings deposited by suspension plasma spraying," *Applied Surface Science*, vol. 439, pp. 60–65, 2018.
- [75] P. Karami, S. Salkhi Khasraghi, M. Hashemi, S. Rabiei, and A. Shojaei, "Polymer/nanodiamond composites- a comprehensive review from synthesis and fabrication to properties and applications," *Advances in Colloid and Interface Science*, vol. 269, pp. 122–151, 2019.
- [76] J. Wang, F.-L. Zhang, T. Zhang, W.-G. Liu, W.-X. Li, and Y.-M. Zhou, "Preparation of Ni-P-diamond coatings with dry friction characteristics and abrasive wear resistance," *International Journal of Refractory Metals and Hard Materials*, vol. 70, pp. 32–38, 2018.
- [77] D. J. Woo, F. C. Heer, L. N. Brewer, J. P. Hooper, and S. Osswald, "Synthesis of nanodiamond-reinforced aluminum metal matrix composites using cold-spray deposition," *Carbon*, vol. 86, pp. 15–25, 2015.
- [78] V. A. Popov, E. V. Shelekhov, A. S. Prosviryakov et al., "Application of nanodiamonds for in situ synthesis of TiC reinforcing nanoparticles inside aluminium matrix during mechanical alloying," *Diamond and Related Materials*, vol. 75, pp. 6–11, 2017.
- [79] V. A. Popov, M. Burghammer, M. Rosenthal, and A. Kotov, "In situ synthesis of TiC nano-reinforcements in aluminum matrix composites during mechanical alloying," *Composites Part B: Engineering*, vol. 145, pp. 57–61, 2018.
- [80] V. Ferreira, P. Egizabal, V. Popov et al., "Lightweight automotive components based on nanodiamond-reinforced aluminium alloy: a technical and environmental evaluation," *Diamond and Related Materials*, vol. 92, pp. 174–186, 2019.
- [81] V. Livramento, J. B. Correia, N. Shohoji, and E. Ōsawa, "Nanodiamond as an effective reinforcing component for nano-copper," *Diamond and Related Materials*, vol. 16, no. 2, pp. 202–204, 2007.
- [82] A. Nieto, J. Kim, O. V. Penkov, D.-E. Kim, and J. M. Schoenung, "Elevated temperature wear behavior of thermally sprayed WC-Co/nanodiamond composite coatings," *Surface and Coatings Technology*, vol. 315, pp. 283–293, 2017.
- [83] A. Loganathan, S. Rengifo, A. F. Hernandez, C. Zhang, and A. Agarwal, "Effect of nanodiamond reinforcement and heat-treatment on microstructure, mechanical and tribological properties of cold sprayed aluminum coating," *Surface and Coatings Technology*, vol. 412, Article ID 127037, 2021.
- [84] K. Yang, X. Shi, A. Zhang, Z. Wang, and Y. Wang, "Effect of multiwalled carbon nanotubes on the lubricating property of TiAl-Ag composite based on the changes in applied loads and testing temperatures," *RSC Advances*, vol. 6, no. 78, pp. 74269–74277, 2016.
- [85] A. Leyland and A. Matthews, "On the significance of the H/E ratio in wear control: a nanocomposite coating approach to optimised tribological behaviour," *Wear*, vol. 246, no. 1–2, pp. 1–11, 2000.
- [86] S. Zhang, Z. Chen, P. Wei et al., "Wear properties of graphene/zirconia biphasic nano-reinforced aluminium matrix composites prepared by SLM," *Materials Today Communications*, vol. 30, Article ID 103009, 2022.
- [87] O. P. Tchernogorova, O. A. Bannykh, V. M. Blinov, E. I. Drozdova, A. A. Dityat'ev, and N. N. Mel'nik, "Superhard carbon particles forming from fullerites in a mixture with iron powder," *Materials Science and Engineering: A*, vol. 299, no. 1–2, pp. 136–140, 2001.
- [88] R. K. Upadhyay and A. Kumar, "A novel approach to minimize dry sliding friction and wear behavior of epoxy by infusing fullerene C70 and multiwalled carbon nanotubes," *Tribology International*, vol. 120, pp. 455–464, 2018.
- [89] T. Hisakado and A. Kanno, "Effects of fullerene C<sub>60</sub> on the friction and wear characteristics of ceramics in ethanol," *Tribology International*, vol. 32, no. 7, pp. 413–420, 1999.
- [90] M. Elhefnawy, G. L. Shuai, Z. Li, D. T. Zhang, M. M. Tawfik, and L. Li, "On achieving ultra-high strength and improved wear resistance in Al-Zn-Mg alloy via ECAP," *Tribology International*, vol. 163, Article ID 107188, 2021.
- [91] Y. Wang, C. Wu, L. Zhang, P. Qu, S. Li, and Z. Jiang, "Thermal oxidation and its effect on the wear of Mg alloy AZ31B," *Wear*, vol. 476, Article ID 203673, 2021.

- [92] M. E. Turan, Y. Sun, and Y. Akgul, "Mechanical, tribological and corrosion properties of fullerene reinforced magnesium matrix composites fabricated by semi powder metallurgy," *Journal of Alloys and Compounds*, vol. 740, pp. 1149–1158, 2018.
- [93] X. Liu, X. Shi, G. Lu et al., "The synergistic lubricating mechanism of Sn-Ag-Cu and C60 on the worn surface of M50 self-lubricating material at elevated loads," *Journal of Alloys and Compounds*, vol. 777, pp. 271–284, 2019.
- [94] Y. Meng, J. Sun, J. He, F. Yang, and P. Wu, "Interfacial interaction induced synergistic lubricating performance of MoS<sub>2</sub> and SiO<sub>2</sub> composite nanofluid," *Colloids and Surfaces A: Physicochemical and Engineering Aspects*, vol. 626, Article ID 126999, 2021.
- [95] S. K. Soni, B. Thomas, and V. R. Kar, "A comprehensive review on CNTs and CNT-reinforced composites: syntheses, characteristics and applications," *Materials Today Communications*, vol. 25, Article ID 101546, 2020.
- [96] J. Qin, C. Wang, Z. Yao et al., "Growing carbon nanotubes on continuous carbon fibers to produce composites with improved interfacial properties: a step towards commercial production and application," *Composites Science and Technology*, vol. 211, Article ID 108870, 2021.
- [97] G. R. Bardajee, M. Sharifi, H. Torkamani, and C. Vancaeyzeele, "Synthesis of magnetic multi walled carbon nanotubes hydrogel nanocomposite based on poly (acrylic acid) grafted onto salep and its application in the drug delivery of tetracycline hydrochloride," *Colloids and Surfaces A: Physicochemical and Engineering Aspects*, vol. 616, Article ID 126350, 2021.
- [98] S. Kumar, Twinkle, and M. Kaur, "Carbon nanotube-derived highly conductive graphene nanoribbons for electronic applications," *Materials Chemistry and Physics*, vol. 259, Article ID 123967, 2021.
- [99] L. C. Zhang, I. Zarudi, and K. Q. Xiao, "Novel behaviour of friction and wear of epoxy composites reinforced by carbon nanotubes," *Wear*, vol. 261, no. 7–8, pp. 806–811, 2006.
- [100] O. Aranke, C. Gandhi, N. Dixit, and P. Kuppan, "Influence of multiwall carbon nanotubes (MWCNT) on wear and coefficient of friction of aluminium (Al 7075) metal matrix Composite," *Materials Today: Proceedings*, vol. 5, no. 2, Part 2, pp. 7748–7757, 2018.
- [101] O. Aranke, C. Gandhi, N. Dixit, and P. Kuppan, "Influence of multiwall carbon nanotubes (MWCNT) on wear and coefficient of friction of aluminium (Al 7075) metal matrix composite," *Materials Today: Proceedings*, vol. 5, no. 2, pp. 7748–7757, 2018.
- [102] S. Lamnini, C. Balázs, and K. Balázs, "Wear mechanism of spark plasma sintered MWCNTs reinforced zirconia composites under dry sliding conditions," *Wear*, vol. 430–431, pp. 280–289, 2019.
- [103] C. Wang, B. Dong, G.-Y. Gao, M.-W. Xu, and H.-L. Li, "A study on microhardness and tribological behavior of carbon nanotubes reinforced AMMA-CNTs copolymer nanocomposites," *Materials Science and Engineering: A*, vol. 478, no. 12, pp. 314–318, 2008.
- [104] R. M. Kumar, S. K. Sharma, B. V. Manoj Kumar, and D. Lahiri, "Effects of carbon nanotube aspect ratio on strengthening and tribological behavior of ultra high molecular weight polyethylene composite," *Composites Part A: Applied Science and Manufacturing*, vol. 76, pp. 62–72, 2015.
- [105] C. Wang, B. Dong, G.-Y. Gao, M.-W. Xu, and H.-L. Li, "A study on microhardness and tribological behavior of carbon nanotubes reinforced AMMA-CNTs copolymer nanocomposites," *Materials Science and Engineering: A*, vol. 478, no. 1–2, pp. 314–318, 2008.
- [106] A. Golchin, A. Wikner, and N. Emami, "An investigation into tribological behaviour of multi-walled carbon nanotube/graphene oxide reinforced UHMWPE in water lubricated contacts," *Tribology International*, vol. 95, pp. 156–161, 2016.
- [107] H. Zhang, B. Zhang, Q. Gao, J. Song, and G. Han, "A review on microstructures and properties of graphene-reinforced aluminum matrix composites fabricated by friction stir processing," *Journal of Manufacturing Processes*, vol. 68, Part B, pp. 126–135, 2021.
- [108] E. Mudra, I. Shepa, M. Hrubovcakova et al., "Highly wear-resistant alumina/graphene layered and fiber-reinforced composites," *Wear*, vol. 484–485, Article ID 204026, 2021.
- [109] T. Ouyang, Y. Shen, R. Yang et al., "3D hierarchical porous graphene nanosheets as an efficient grease additive to reduce wear and friction under heavy-load conditions," *Tribology International*, vol. 144, Article ID 106118, 2020.
- [110] Z. Xu, X. Shi, W. Zhai, J. Yao, S. Song, and Q. Zhang, "Preparation and tribological properties of TiAl matrix composites reinforced by multilayer graphene," *Carbon*, vol. 67, pp. 168–177, 2014.
- [111] W. Zhai, L. Bai, R. Zhou et al., "Recent progress on wear-resistant materials: designs, properties, and applications," *Advanced Science*, vol. 8, no. 11, Article ID 2003739, 2021.
- [112] Y. Liu, X. Liu, X. Zhang et al., "Tribological properties and self-lubrication mechanism of in-situ grown graphene reinforced nickel matrix composites in ambient air," *Wear*, vol. 496–497, Article ID 204308, 2022.
- [113] A. K. Krella, "Cavitation erosion of monolayer PVD coatings – an influence of deposition technique on the degradation process," *Wear*, vol. 478–479, Article ID 203762, 2021.
- [114] R. K. Upadhyay and A. Kumar, "Effect of humidity on the synergy of friction and wear properties in ternary epoxy-graphene-MoS<sub>2</sub> composites," *Carbon*, vol. 146, pp. 717–727, 2019.
- [115] L. Liu, Z. Wang, Y. Yu et al., "Engineering interfaces toward high-performance polypropylene/coir fiber biocomposites with enhanced friction and wear behavior," *ACS Sustainable Chemistry and Engineering*, vol. 7, no. 22, pp. 18453–18462, 2019.
- [116] K. Xie, B. Cai, G. Zhang et al., "High-strength Al matrix composites reinforced with uniformly dispersed nanodiamonds," *Journal of Alloys and Compounds*, vol. 898, Article ID 162917, 2022.
- [117] Y. J. Huang, F. L. Zhang, M. J. Zhai, M. X. Zhu, and D. L. Xie, "Mechanical properties and tribological behavior of Fe/nanodiamond composite prepared by hot-press sintering," *International Journal of Refractory Metals and Hard Materials*, vol. 95, Article ID 105412, 2020.
- [118] R. K. Upadhyay and A. Kumar, "A novel approach to minimize dry sliding friction and wear behavior of epoxy by infusing fullerene C<sub>70</sub> and multiwalled carbon nanotubes," *Tribology International*, vol. 120, pp. 455–468, 2018.
- [119] H. J. Choi, S. M. Lee, and D. H. Bae, "Wear characteristic of aluminum-based composites containing multi-walled carbon nanotubes," *Wear*, vol. 270, no. 1–2, pp. 12–18, 2010.
- [120] W. Man, Y. Huang, H. Gou, Y. Li, J. Zhao, and Y. Shi, "Synthesis of novel CuO@Graphene nanocomposites for lubrication application via a convenient and economical method," *Wear*, vol. 498–499, Article ID 204323, 2022.
- [121] S. Farhad, F. Zhang, S. Liu, and T. Liu, "Tribological properties, thermal conductivity and corrosion resistance of

- titanium/nanodiamond nanocomposites,” *Composites Communications*, vol. 10, pp. 57–63, 2018.
- [122] A. Diez-Ibarbia, A. Fernandez-del-Rincon, P. Garcia, and F. Viadero, “Gear rattle dynamics under non-stationary conditions: The lubricant role,” *Mechanism and Machine Theory*, vol. 151, Article ID 103929, 2020.
- [123] R. Kumar, H. Kumar Banga, H. Singh, and S. Kundal, “An outline on modern day applications of solid lubricants,” *Materials Today: Proceedings*, vol. 28, Part 3, pp. 1962–1967, 2020.
- [124] M. Zhou, J. Guo, L. P. Guo, and J. Bai, “Electrochemical sensing platform based on the highly ordered mesoporous carbon-fullerene system,” *Analytical Chemistry*, vol. 80, no. 12, pp. 4642–4650, 2008.
- [125] Y. Wu, X. Yang, W. Chen et al., “Perovskite solar cells with 18.21% efficiency and area over 1 cm<sup>2</sup> fabricated by heterojunction engineering,” *Nature Energy*, vol. 1, Article ID 16148, 2016.
- [126] B. André, F. Gustavsson, F. Svahn, and S. Jacobson, “Performance and tribofilm formation of a low-friction coating incorporating inorganic fullerene like nano-particles,” *Surface and Coatings Technology*, vol. 206, no. 8–9, pp. 2325–2329, 2012.
- [127] J. Lee, S. Cho, Y. Hwang et al., “Application of fullerene-added nano-oil for lubrication enhancement in friction surfaces,” *Tribology International*, vol. 42, no. 3, pp. 440–447, 2009.
- [128] B.-C. Ku, Y.-C. Han, J.-E. Lee, J.-K. Lee, S.-H. Park, and Y.-J. Hwang, “Tribological effects of fullerene (C<sub>60</sub>) nanoparticles added in mineral lubricants according to its viscosity,” *International Journal of Precision Engineering and Manufacturing*, vol. 11, pp. 607–611, 2010.
- [129] F. A. Yunusov, A. D. Breki, E. S. Vasilyeva, and O. V. Tolochko, “The influence of nano additives on tribological properties of lubricant oil,” *Materials Today: Proceedings*, vol. 30, Part 3, pp. 632–634, 2020.
- [130] B. S. A. Vardhaman, M. Amarnath, J. Ramkumar, and K. Mondal, “Enhanced tribological performances of zinc oxide/MWCNTs hybrid nanomaterials as the effective lubricant additive in engine oil,” *Materials Chemistry and Physics*, vol. 253, Article ID 123447, 2020.
- [131] L. Liu, Z. Fang, A. Gu, and Z. Guo, “Lubrication effect of the paraffin oil filled with functionalized multiwalled carbon nanotubes for bismaleimide resin,” *Tribology Letters*, vol. 42, pp. 59–65, 2011.
- [132] P. Nie, C. Min, H.-J. Song, X. Chen, Z. Zhang, and K. Zhao, “Preparation and tribological properties of polyimide/carboxyl-functionalized multi-walled carbon nanotube nanocomposite films under seawater lubrication,” *Tribology Letters*, vol. 58, Article ID 7, 2015.
- [133] C. Min, D. Liu, Z. He, S. Li, Z. Kan, and Y. Huang, “Preparation of novel polyimide nanocomposites with high mechanical and tribological performance using covalent modified carbon nanotubes via Friedel–Crafts reaction,” *Polymer*, vol. 150, pp. 223–231, 2018.
- [134] X. Ye, E. Songfeng, and M. Fan, “The influences of functionalized carbon nanotubes as lubricating additives: length and diameter,” *Diamond and Related Materials*, vol. 100, Article ID 107548, 2019.
- [135] N. Sharma, N. A. Syed, B. C. Ray, S. Yadav, and K. Biswas, “Wear behaviour of silica and alumina-based nanocomposites reinforced with multi walled carbon nanotubes and graphene nanoplatelets,” *Wear*, vol. 418–419, pp. 290–304, 2019.
- [136] Y. Peng, Y. Hu, and W. Hui, “Tribological behaviors of surfactant-functionalized carbon nanotubes as lubricant additive in water,” *Tribology Letters*, vol. 25, pp. 247–253, 2007.
- [137] A. Javeed, B. John, and A. P. Mana, “Tribological performance of engine oil with graphene oxide nano additives on cylinder liner honing surface at high contact pressure,” *Materials Today: Proceedings*, vol. 45, Part 4, pp. 4008–4011, 2021.
- [138] P. Guo, L. Chen, J. Wang, Z. Geng, Z. Lu, and G. Zhang, “Enhanced tribological performance of aminated nano-silica modified graphene oxide as water-based lubricant additive,” *ACS Applied Nano Materials*, vol. 1, no. 11, pp. 6444–6453, 2018.
- [139] H. Xie, B. Jiang, J. Dai et al., “Tribological behaviors of graphene and graphene oxide as water-based lubricant additives for magnesium alloy/steel contacts,” *Materials*, vol. 11, no. 2, Article ID 206, 2018.
- [140] H. Kinoshita, Y. Nishina, A. A. Alias, and M. Fujii, “Tribological properties of monolayer graphene oxide sheets as water-based lubricant additives,” *Carbon*, vol. 66, pp. 720–723, 2014.
- [141] R. Mirzaamiri, S. Akbarzadeh, S. Ziaei-Rad, D.-G. Shin, and D.-E. Kim, “Molecular dynamics simulation and experimental investigation of tribological behavior of nanodiamonds in aqueous suspensions,” *Tribology International*, vol. 156, Article ID 106838, 2021.
- [142] W. Zhai, W. Lu, X. Liu, and L. Zhou, “Nanodiamond as an effective additive in oil to dramatically reduce friction and wear for fretting steel/copper interfaces,” *Tribology International*, vol. 129, pp. 75–81, 2019.
- [143] A. Golchin, A. Villain, and N. Emami, “Tribological behaviour of nanodiamond reinforced UHMWPE in water-lubricated contacts,” *Tribology International*, vol. 110, pp. 195–200, 2017.
- [144] O. Elomaa, T. J. Hakala, V. Myllymäki et al., “Diamond nanoparticles in ethylene glycol lubrication on steel–steel high load contact,” *Diamond and Related Materials*, vol. 34, pp. 89–94, 2013.
- [145] P. Wu, X. Chen, C. Zhang, and J. Luo, “Synergistic tribological behaviors of graphene oxide and nanodiamond as lubricating additives in water,” *Tribology International*, vol. 132, pp. 177–184, 2019.
- [146] M. Hirano and K. Shinjo, “Atomistic locking and friction,” *Physical Review B*, vol. 41, no. 17, Article ID 11837, 1990.
- [147] J. Hua, M. Björling, R. Larsson, and Y. Shi, “Controllable superlubricity achieved with mixtures of green ionic liquid and glycerol aqueous solution via humidity,” *Journal of Molecular Liquids*, vol. 345, Article ID 117860, 2022.
- [148] H. Shekhar and R. Dumpala, “Overcoming friction and steps towards superlubricity: a review of underlying mechanisms,” *Applied Surface Science Advances*, vol. 6, Article ID 100175, 2021.
- [149] H. Bai, H. Bao, Y. Li, H. Xu, S. Li, and F. Ma, “Moiré pattern based universal rules governing interfacial superlubricity: a case of graphene,” *Carbon*, vol. 191, pp. 28–35, 2022.
- [150] L. Van Sang, N. Sugimura, and H. Washizu, “Graphene as solid lubricant vertically buried into iron contact surface by annealing for superlubricity,” *Tribology International*, vol. 165, Article ID 107288, 2022.
- [151] R. Li, X. Yang, D. Hou, Y. Wang, and J. Zhang, “Superlubricity of carbon nanostructural films enhanced by graphene nanoscrolls,” *Materials Letters*, vol. 271, Article ID 127748, 2020.

- [152] S. Shi, D. Guo, and J. Luo, "Micro/atomic-scale vibration induced superlubricity," *Friction*, vol. 9, pp. 1163–1174, 2021.
- [153] D. Peng, J. Wang, H. Jiang et al., "100 km wear-free sliding achieved by microscale superlubric graphite/DLC heterojunctions under ambient conditions," *National Science Review*, vol. 9, no. 1, Article ID nwab109, 2022.
- [154] Z. Gong, C. Bai, L. Qiang, K. Gao, J. Zhang, and B. Zhang, "Onion-like carbon films endow macro-scale superlubricity," *Diamond and Related Materials*, vol. 87, pp. 172–176, 2018.
- [155] H. Li and P. S. Branicio, "Ultra-low friction of graphene/C<sub>60</sub>/graphene coatings for realistic rough surfaces," *Carbon*, vol. 152, pp. 727–737, 2019.
- [156] J. Li, Y. Peng, X. Tang, Q. Xu, and L. Bai, "Effect of strain engineering on superlubricity in a double-walled carbon nanotube," *Physical Chemistry Chemical Physics*, vol. 23, no. 8, pp. 4988–5000, 2021.
- [157] A. Kis, K. Jensen, S. Aloni, W. Mickelson, and A. Zettl, "Interlayer forces and ultralow sliding friction in multiwalled carbon nanotubes," *Physical Review Letters*, vol. 97, no. 2, Article ID 025501, 2006.
- [158] H. Xu, J. Al-Ghalith, and T. Dumitrică, "Smooth sliding and superlubricity in the nanofriction of collapsed carbon nanotubes," *Carbon*, vol. 134, pp. 531–535, 2018.
- [159] Y. Wang, K. Gao, B. Zhang, Q. Wang, and J. Zhang, "Structure effects of sp<sup>2</sup>-rich carbon films under super-low friction contact," *Carbon*, vol. 137, pp. 49–56, 2018.
- [160] Z. Gong, J. Shi, B. Zhang, and J. Zhang, "Graphene nano scrolls responding to superlow friction of amorphous carbon," *Carbon*, vol. 116, pp. 310–317, 2017.
- [161] E. Lewin, B. André, S. Urbonaite, U. Wiklund, and U. Jansson, "Synthesis, structure and properties of Ni-alloyed TiC<sub>x</sub>-based thin films," *Journal of Materials Chemistry*, vol. 20, no. 28, pp. 5950–5960, 2010.
- [162] A. Erdemir, "The role of hydrogen in tribological properties of diamond-like carbon films," *Surface and Coatings Technology*, vol. 146–147, pp. 292–297, 2001.
- [163] G. Ru, W. Qi, K. Tang, Y. Wei, and T. Xue, "Interlayer friction and superlubricity in bilayer graphene and MoS<sub>2</sub>/MoSe<sub>2</sub> van der Waals heterostructures," *Tribology International*, vol. 151, Article ID 106483, 2020.
- [164] Y. Liu, J. Li, X. Ge et al., "Macroscale superlubricity achieved on the hydrophobic graphene coating with glycerol," *ACS Applied Materials and Interfaces*, vol. 12, no. 16, pp. 18859–18869, 2020.
- [165] Z. Chen, Y. Liu, and J. Luo, "Superlubricity of nanodiamonds glycerol colloidal solution between steel surfaces," *Colloids and Surfaces A: Physicochemical and Engineering Aspects*, vol. 489, pp. 400–406, 2016.
- [166] S. Mia and N. Ohno, "Prediction of pressure–viscosity coefficient of lubricating oils based on sound velocity," *Lubrication Science*, vol. 21, no. 9, pp. 343–354, 2009.
- [167] D. Dowson and Z.-M. Jin, "Metal-on-metal hip joint tribology," *Proceedings of the Institution of Mechanical Engineers, Part H: Journal of Engineering in Medicine*, vol. 220, no. 2, pp. 107–118, 2006.
- [168] N. Shao, Y. Gao, and X. C. Zeng, "Search for lowest-energy fullerenes 2: C<sub>38</sub> to C<sub>80</sub> and C<sub>112</sub> to C<sub>120</sub>," *The Journal of Physical Chemistry C*, vol. 111, no. 48, pp. 17671–17677, 2007.